ISTANBUL TECHNICAL UNIVERSITY ★ GRADUATE SCHOOL OF SCIENCE ENGINEERING AND TECHNOLOGY

STABILITY CONTROL PROBLEM FOR SPACE VEHICLES WITH FUEL SLOSH

M.Sc. THESIS

Merve ŞAHİN

Department of Aeronautical and Astronautical Engineering

Aeronautical and Astronautical Engineering Programme

JUNE 2015

ISTANBUL TECHNICAL UNIVERSITY ★ GRADUATE SCHOOL OF SCIENCE ENGINEERING AND TECHNOLOGY

STABILITY CONTROL PROBLEM FOR SPACE VEHICLES WITH FUEL SLOSH

M.Sc. THESIS

Merve ŞAHİN
511121176

Department of Aeronautical and Astronautical Engineering

Aeronautical and Astronautical Engineering Programme

Thesis Advisor: Prof. Dr. Metin Orhan KAYA

JUNE 2015

<u>İSTANBUL TEKNİK ÜNİVERSİTESİ ★ FEN BİLİMLERİ ENSTİTÜSÜ</u>

YAKIT ÇALKALANMALI UZAY ARAÇLARI İÇİN STABİLİTE KONTROL PROBLEMİ

YÜKSEK LİSANS TEZİ

Merve ŞAHİN
511121176

Uçak ve Uzay Mühendisliği Anabilim Dalı

Uçak ve Uzay Mühendisliği Programı

Tez Danışmanı: Prof. Dr. Metin Orhan KAYA

HAZİRAN 2015

Merve ŞAHİN, a **M.Sc**. student of ITU **Graduate School of Science Engineering and Technology** 511121176 successfully defended the thesis entitled **"STABILITY CONTROL PROBLEM FOR SPACE VEHICLES WITH FUEL SLOSH"**, which she prepared after fulfilling the requirements specified in the associated legislations, before the jury whose signatures are below.

Thesis Advisor :	**Prof. Dr. Metin Orhan KAYA** Istanbul Technical University	....
Jury Members :	**Prof. Dr. Erol UZAL** Istanbul University	....
	Ass. Prof. Dr. Özge ÖZDEMİR Istanbul Technical University	....

Date of Submission : 04 May 2015
Date of Defense : 04 June 2015

To my parents and lovely brother,

FOREWORD

First and foremost, the research and accomplishment of this thesis would not have been possible without the support and guidance of my advisor Prof. Dr. Metin Orhan KAYA. I would like to thank him for giving me valuable advice and support when needed.

Special thanks also go to my parents, Erol and Serpil and to my dearie brother, Burak for their unconditional love and support through all my life.

June 2015 Merve ŞAHİN
(Physicists)

TABLE OF CONTENTS

Page

ABBREVIATIONS

AVUM	**:** Attitude Vernier Upper Module
CFD	**:** Computational Fluid Dynamics
kg	**:** Kilogram
LNG	**:** Liquified Natural Gas
LQR	**:** Linear Quadratic Regulator
m	**:** Meter
N	**:** Newton
NASA	**:** National Aeronautics and Space Administration
rad	**:** Radian
s	**:** Second
t	**:** Time
$\mathbf{t_b}$	**:** Fuel burn time

LIST OF TABLES

Page

LIST OF FIGURES

Page

STABILITY CONTROL PROBLEM FOR SPACE VEHICLES WITH FUEL SLOSH

SUMMARY

Sloshing is caused by any disturbance of free liquid surface in a partially filled tank. Depending on the peak accelerations in any direction or the shape of container, the free surface of liquid can be subjected to different types of motion either symmetric or asymmetric. These types of motion have significant influence on vehicles which have liquid fuel in their tanks. Owing to the fact that fuel sloshing plays a crucial role in the stability of the vehicles, many diversified engineering departments give considerable attention to this problem. To prevent structural damages for vehicles with liquid fuel such as trucks on highways, cars, ships, space vehicles, new designs of tanks are evaluated and loss of the stability due to sloshing is tried to minimise. To prevent sloshing effects, physical barriers are placed into the fuel tank such as baffles or containers are designed by using bladders. Main purpose of these designes is to limit the movement of liquid fuel. But these techniques increase both the mission cost and the weight of the tank of spacecraft.

The natural frequency of motion of liquid is related to two main factors (i) the shape of tank and (ii) the acceleration of gravity or the axial acceleration of vehicle. A liquid's motion contains an infinite number of natural frequencies, however the lowest few modes of frequencies are the most important for vehicle. When the natural frequency of liquid fuel coincides with the frequency of the vehicle, this situation generates resonance and damages the structure. Near resonance, the fluid's motion loses linearity and nonlinear representation starts to be valid.

An analytical approach to sloshing has some limits to obtain a solution. Factors like tank shape, existence of external forces etc. have a great importance to design a model for sloshing phenomena. By taking into consideration the factors, to use an equivalent mechanical model becomes a realistic approach to liquid dynamics in closed tanks. Primal parameters of liquid are qualified and by utilizing these parameters, equivalent mechanical models are designed. Some rules must be followed before equivalent mechanical models are created. Firstly, passing from the liquid material to rigid masses, the change of masses and moments of inertia must be preserved. Then, center of gravity must be unchangeable. The equivalent models produce the same frequency range as liquid model does. Lastly, the system must come up with the results which is equivalent to real material. Having regard to these conditions, physical parameters must be determined, then the system is designed.

The major objective of this thesis is to investigate the case of sloshing in space vehicles by utilizing equivalent mechanical models. Mass-spring system is one of the models, and for small oscillations, it becomes the most appropriate model. It replaces the liquid fuel by becoming inner-rigid-masses corresponding to first few slosh modes. As a result of axial and transverse accelerations of space vehicle, the inner-masses begin to

oscillate and have a great impression on the stability of vehicle. After designing an acceptable model, to investigate the stability, optimal feedback law and Lyapunov-based control law are utilized. Firstly, the model is designed with two-inner-masses and the results of simulations are demonstrated. Then, the model with four-inner-masses are designed and same steps are applied to it in order to show the stability of the spacecraft.

When large-amplitude oscillations occur, mass-spring system is no longer sufficient to demonstrate the change in the stability of spacecraft. In such a case, simple-pendulum model accommodates to the circumstances and describes relatively large motions. For sloshing due to a nonplanar or rotational motion, simple-pendulum model fits to real life cases excellently.

The main purpose is to derive the equations of motion of spacecraft by means of these two model. Utilizing the mass-spring-system and simple-pendulum model, the motion of vehicle in a specific time and plane can be estimated. Moreover, the stability of the space vehicle can be investigated by taking advantages of Linear Quadratic Regulator and Lyapunov-based control laws.

Apart from these two cases, space vehicle is investigated under lateral and pitching excitations. The equations of motion are derived by using the same parameters and they are compared to each other. In previous models, it is assumed that there are no external forces or moments. But in these models, important thing is the change of force and moment equations for either mass-spring system or simple-pendulum system under excitations. Moreover, in these systems, gravitational effects are not neglected.

YAKIT ÇALKALANMALI UZAY ARAÇLARI İÇİN STABİLİTE KONTROL PROBLEMİ

ÖZET

Yakıt çalkalanmasına, hareket eden bir aracın kısmen dolu olan yakıt tankında ki sıvının serbest yüzeyinin düzeninin bozulması sebep olur. Herhangi bir yöndeki ani ivmelenmeye ya da konteyner şekline bağlı olarak, sıvının serbest yüzeyi simetrik ya da simetrik olmayan birçok farklı hareket tipine maruz kalabilir. Bu hareket tipleri, tanklarında sıvı yakıt bulunduran araçlar üzerinde kayda değer bir etkiye sahiptir. Yakıt çalkalanmasının araç stabilitesi üzerinde hayati bir rolü olduğundan dolayı, birçok mühendislik bölümü bu probleme hatırı sayılır derecede önem vermektedir. Otoyollardaki kamyonlar, arabalar, gemiler, uzay araçları gibi sıvı yakıtlı araçlar için yapısal zararı önlemek adına yakıt tankları için yeni modeller tasarlanmaktadır ve çalkalanmadan kaynaklanan stabilite kaybı en aza indirilmeye çalışılmaktadır. Bu çalkalanmayı önlemek adına tank içine yönlendirici fiziksel bariyerler yerleştirilmekte ya da tank keseli bir şekilde dizayn edilmektedir. Tüm bu tasarımların amacı yakıt çalkalanması sonucu çıkabilecek hareket tiplerini kısmen de olsa engellemek ve sınırlamaktır. Fakat bu yöntemler, hem görev maliyetini fazlalaştırmakta hem de tankın kütlesini artırmaktadır.

Sıvının hareketinin doğal frekansı, hareketi tayin etmede önemlidir ve iki ana etkene bağlıdır; (i) tankın şekli ve (ii) yer çekimi ivmesi ya da aracın eksenel ivmesi. Bir sıvının hareketi sonsuz sayıda doğal frekans modları içerir, fakat araç için önemli olan aralık en düşük bir kaç frekans modudur. İlk frekans modlarından sonra aracın hareketine bağlı olarak sıvının davranışı kaosa doğru gidebilir. Bunun yanı sıra sıvının doğal frekansı aracın frekansıyla çakıştığında, bu durum rezonans oluşmasına sebep olur ve yapıya zarar verir. Rezonans kaynaklı yapısal zararlar geri dönüşü olmayan bir biçimde araca zarar verir, sıvı yakıtlı tanklarda patlamaya bile yol açabilir. Çünkü rezonans aralığı yakınlarında, akışkanın hareketi lineerlikten uzaklaşır ve lineer olmayan bir temsil geçerli olmaya başlar ve sıvının hareketi tayin edilemez bir duruma gelir. Bundan dolayı tasarım yapılırken lineer ya da lineer olmayan durum göz önünde bulundurulmalı ve bu duruma uygun modellere başvurulmalıdır.

Probleme bir çözüm elde etmek için yakıt çalkalanmasına analitik olarak yaklaşmanın bazı sınırları vardır. Tank şekli, dışsal kuvvetlerin var oluşu vb. etkenler çalkalanma olayı için model tasarlarken önemli bir etkiye sahiptir. Sıvı hareketi oldukça belirsizdir ve öngörülmesi zor bir yol izler. Bundan dolayı bu etkenleri dikkate alarak, sıvı yakıta denk olarak tasarlanan bir mekanik model kapalı tanklarda gerçekci bir yaklaşım olarak görülür. Sıvının başlıca parametreleri belirlenir ve bu parametrelerden yararlanarak eş değer mekanik modeller dizayn edilir.Bu mekanik modeller tasarlanmadan önce uyulması gereken bir takım kurallar vardır. Sıvıdan katı kütleli modellere geçerken öncelikle kütle ve eylemsizlik momenti korunmalıdır. Ardından ağırlık merkezi, tasarım yaptıktan sonra küçük salınımlar için bile değişmeyecek bir şekilde ayarlanmalıdır. Sistem dizayn edildikten sonra sıvı yakıtlı halinde ki titreşim

modlarına sahip olmalı ve aynı sönümlü kuvveti üretmelidir. Son olarak sistem, dışardan bir rahatsızlık varolduğunda gerçek model tarafından üretilebilecek sonuçlara denk olarak bir sonuç üretmelidir. Tüm bunlar göz önüne alındıktan sonra fiziksel parametreler belirlenmeli ve sistem ona göre tasarlanmalıdır.

Bu tezin başlıca amacı, yukarı da belirtildiği gibi uzay araçlarında ki yakıt çalkalanmasını sıvıya eş değer olarak modellenen mekanik sistemleri kullanarak incelemektir. Bu modelleri uygulamanın en büyük sebebi, kuru yüklerin hareketlerinin sıvı yüklerin hareketlerinden daha tahmin edilebilir olması ve sıvı yükün hareket karmaşasını en aza indirgemektir. Bu çalışmada kütle-yay sistemi bu amaçla kullanılan modellerden birisidir ve küçük salınımlar için en uygun modeldir. Ilk bir kaç çalkalanma moduna karşılık olarak oluşturulan iç-katı-kütleler sıvı yakıtla yer değişir. Uzay aracının eksenel ve enine ivmelerinin bir sonucu olarak, iç-kütleler salınım yapmaya başlarlar ve aracın hareket kararlılığında oldukça büyük etkiye sahip olurlar. Uygun ve kabul edilebilir bir model tasarlandıktan sonra, aracın hareketinde ki değişimleri görebilmek adına bir takım kontrol yasalarından yararlanılır ki bunlar optimal geri besleme kontrol yasası ve Lyapunov temelli kontrol yasalarıdır. Kütle-yay modeli tasarlanırken iç-kütleleri farklı sayıda kullanıp sonuç görmek adına öncelikle iki-iç-kütleli model tasarlanır. Bu model esas alınarak aracın stabilitesi incelenir, kütlelerin yer değişimlerinin yanı sıra eksenel hız, yunuslama momenti ve sapma açısı grafiklerle gösterilir. Bu modelin ardından dört-iç-kütleli yeni bir model kurulur ve bir önceki model ile karşılaştırılmak için sistem aynı işlemlerden geçirilir. Stabilite incelenir ve kütlelerin yer değişim miktarı, eksenel hız, yunuslama momenti ve sapma açısı bu model için de bulunur. Ardından iç-kütle sayısında ki değişimin araç stabilitesini tayin etmede etkin bir rolü olup olmadığı modeller karşılaştırılarak bulunur.

Aracın hareketine bağlı olarak büyük genlikli salınımlar meydana geldiğinde, kütle-yay sistemi aracın stabilitesinde ki değişimi gösterebilecek kadar yeterli olmaz. Böyle bir durumda, basit-sarkaç modeli koşullara uyum sağlar ve büyük hareket genliklerini tanımlar. Düzlemsel olmayan ya da rotasyonel hareket sonucu oluşan yakıt çalkalanması için basit-sarkaç modeli gerçeğe en yakın duruma oldukça iyi bir şekilde uymaktadır. Tezin bir kısmında, kütle-yay sistemine benzer parametreler kullanılarak uygun bir basit-sarkaç modeli tasarlanır ve kontrol yasalarından yararlanılarak araç kararlılığı incelenir.

Burada ki asıl amaç uzay aracının hareket denklemlerini bu iki mekanik modeli kullanarak türetmektir. Kütle-yay sisteminden ve basit-sarkaç modelinden yararlanarak, aracın hareket denklemleri belirli bir zaman aralığında ve belirli bir düzlemde elde edilebilir. Buna ek olarak, uzay aracının kararlılığı, bir takım kontrol yasalarından yararlanılarak incelenebilir. Burada kullanılan kontrol yasaları optimal geri besleme kontrol yasası ve Lyapunov temelli kontrol yasasıdır.

Yukarıda bahsedilen kütle-yay sistemi ve basit-sarkaç sistemi incelenirken yer çekimsel etkiler yok sayılır ve dışsal bir kuvvetin olmadığı durumlar incelenir. Simülasyon sonuçları bu şartlar altında elde edilir. Ama daha gerçekci bir model olması açısından gravitasyonel etkileri göz önüne alarak, dış kuvvet ve momentlere maruz kalan modeli incelemek adına, uzay aracı yanal eksenden ve yunuslama doğrultusundan dış uyarıya maruz bırakılır ve bu durum altında aracın hareketi ve tepkisi incelenir. Burada ki önemli nokta aracın kararlılığını sağladığını görebilmektir ve sistemler teorik olarak incelenir. Roketlere ait benzer parametreler kullanılarak hareket denklemleri türetilir ve bu etkiler altında kuvvet ve moment değişimi incelenir.

Lineer modelleme olarak adlandırılan ve yukarıda bahsedilen sistemler birbirlerine tamamen denk olan mekanik modellerdir. Kütle-yay sistemi için belirlenen yay direngenliği basit-sarkaç sisteminde sarkaç ağırlığının uzunluğuna bölümüne karşılık gelir. Her iki modelde belirlenen kütleler birbirlerinden tamamen bağımsız değildirler ve kütle-yay pozisyonu ile basit-sarkaç modelinin pozisyonu göz ardı edilebilecek hata payına sahip bir şekilde saptanabilir. Mekanik modelin avantajı, akışkanın serbest-yüzey hareketini sıvının bir kısmının katı kütle gibi diğer kısmının ise kütle-yay ya da basit-sarkaç sistemi gibi düşünülerek fiziksel bir şekilde yorumlamaya olanak tanımasıdır. Bu lineer modeler, dışarıdan verilen uyarının frekansıyla çalkalanma modal frekansları çakışmadığında ve uyarı genliği oldukça küçük olduğunda ideal davranış sergilerler. Fakat bu durumun tam aksi mevcut olduğunda lineer modeler yerini lineer olmayan modellere bırakmak zorundadır. Bu tez kapsamında frekansların aynı aralıkta olmadığı ve genliklerin küçük olduğu varsayılıp lineer modeller kurulur.

1. INTRODUCTION

There are two kinds of propellant, which are generally used in rockets and missiles, as rigid and liquid. Liquid fuel is used for the first time for a flight of a rocket in the 1920s by Dr. Robert H. Goddard [1]. Since that time, liquid fuel becomes widespread. Because propellant slosh can cause uncertainty in space vehicle's attitude and structural failure of vehicles, sloshing has been severe problem for space vehicles which have liquid propellant in their fuel tanks. Up to the present, the sloshing problem cause several accidents thereby mission failures in space area because most of the space vehicles contain liquid fuel in their tanks as nearly 40% of initial total mass. The studies about sloshing involves very complex mathematical modeling and dynamical analysis in order to avoid slosh effects and find the vehicle structure frequencies.

Sloshing is one of the material effects on the stability of the spacecraft and it takes place when space vehicles have peak acceleration in the take-off time, then the liquid fuel starts to move inside the tank. Two of the components of this peak acceleration, translational and rotational accelerations, produce fuel sloshing. Fig. 1.1 shows a tank with half full liquid propellant under lateral excitation and the first three mode shapes of the fuel.

Figure 1.1: Three modes of sloshing fuel

Effects of the interaction of the movement of propellant with the rigid body can be prevented by using some physical barriers. NASA releases a comprehensive study about slosh suppression in 1969 and from that day to today lots of companies and people try to find avoid sloshing effects [2]. There are several passive techniques such as baffles, bladders and partitions which these physical barriers limit the movement of liquid propellant. Although these techniques have been very effective, yet they do not prevent completely the effects of sloshing and they increase the weight of space vehicles thereby the cost of vehicles.

1.1 Literature Review

Since sloshing adversely affect space vehicle performance, great numbers of problems have been studied so as to see the sloshing effects, limit the movement of liquid etc. Ebrahimian et al. determine an equivalent mechanical model for multi-baffled containers, and the effects of baffles on some parameters are investigated. The model of fluid is developed by using the Laplace equation and Green's theorem and the boundary element method is used to solve the governing equation [3]. One of the principle of the slosh dynamics is to estimate the movement of liquid fuel under the acceleration of vehicle. Based on this, Adler and friends use a laser sensor so as to measure the fluid displacement in the tank and find the natural frequency of sloshing fuel [4].

In the literature of slosh dynamics, to facilitate to determine the equations which belong to liquid, some mechanical models are used such as mass-spring system and simple pendulum model. Dong and his colleagues try to figure out the effect of propellant slosh by using an equivalent mass-spring system and that system is built by use of Computational Fluid Dynamics (CFD) [5]. Dodge and Garza study to show liquid sloshing experimentally and theoretically with a mass-spring model. In the theory part, Bond number is kept at a specific value and the results of high-g conditions and low gravity are compared with each other. The experiments are done by using different liquids in some small tanks. As a result, a correlation is found between the theory and experiments [6]. In any other study, a multi-mass-spring model is used to acquire a nonlinear mathematical model in order to show the slosh modes and Lyapunov-based nonlinear feedback control laws are designed to see the stability of vehicle [7].

In one of the models of simple pendulum, the dynamic model of sloshing under some excitations is developed by using Lagrangian method in order to examine influences over the rocket. The main idea in this study is to focus on the characteristics of weakly nonlinear sloshing [8]. In an article, another simple-pendulum model is used to design the propellant that is within partially filled tank and the model is obtained from calculations about some parameters as the vehicle's lateral acceleration changes. FLUENT is the program being used to obtain sloshing frequency, forces and the other parameters in order to simulate liquid sloshing in the tank [9].

Together with all the theoretical and experimental studies, there are several patents all over the world and one of them belongs to Robert W. Conaway and James S. Spindler about anti slosh media for fuel tanks. This study inserts a baffle system into fuel tanks to prevent sloshing effects. The tank is filled with plastic balls and these balls are designed not to prevent the movement of the liquid but to restrain the sloshing effects [10]. Another patent is anti-sloshing apparatus by Sang-Eon Chun, which effectively prevents sloshing of liquid fuel in any shape and size of tanks for any vehicles such as spacecraft, cars etc. This invention presents anti-sloshing equipment which has buoyancy to be floated on the surface of the liquid to minimize the sloshing effects [11]. Deog Jin Ha has a patent named as anti-sloshing structure for LNG cargo tank to lessen sloshing phenomenon by using two base barriers. In the invention, while the first barrier prevents leakage of liquid fuel, a second barrier becomes a complementary part for the first one and includes anti-sloshing bulkhead to reduce sloshing problem [12]. At last but not least, Bryce Andrew Schwager and Patrick Joseph Curran make a diagnostic mechanism for liquid fuel to attain accurate output signal in order to avoid calculating false indications. This mechanism controls fuel system valves and an electronic controller measures the level of fuel at certain time to see the state of the sloshing [13].

1.2 Purpose of Thesis

The underlying physics of the sloshing effects by investigating the liquid is fairly complex and mistakable. Therefore, this dissertation presents a realistic approximation to the liquid dynamics inside closed containers by utilizing equivalent rigid masses. In this thesis, the main idea is to see fuel-sloshing effects on the stability of the spacecraft. Hence, a mechanical transition is applied to liquid propellant by transforming it into rigid fuel bodies by using equivalent mechanical models such as mass-spring system and simple-pendulum model.

Both mechanical models are investigated theoretically and necessary physical parameters, which are taken from articles by Mahmut Reyhanoglu and Jaime Rubio Hervas, are utilized to control the stability of the spacecraft. In this study, Linear Quadratic Controller and Lyapunov-based controller are chosen as the main controllers to compare results to each other and make a verification for previous works in the literature.

1.3 Overview

This part deals with the whole content of dissertation by giving an outline of each chapter. The general information is given to one who is eager to learn about slosh dynamics and transformations from liquid to rigid masses.

Chapter 2 demonstrates the motion of spacecraft theoretically in the case of lateral and pitching excitations. Force and moment equations are derived under these excitations and compared to each other. For this purpose, two models, which is multi-mass-spring system and multi-simple-pendulum system, are utilized to obtain the changes in moment and force equations of the system.

Chapter 3 is about multi-mass-spring system which is applied to liquid fuel in the tank of AVUM upper stage spacecraft Vega. At first, considering the system, equations of motion are derived by the help of Lagrange equations. Then, the linearized system are acquired and by using these equations, new inputs are determined for feedback controllers and simulations. Optimal feedback control law and Lyapunov-based control law are utilized in order to compare each laws' results about the stability of the spacecraft. In this investigation, it is assumed that there are no external forces and gravitational effects are ignored.

The concept of Chapter 4 is similar to previous chapter in general terms. The model used here is single-simple-pendulum model and the equations of motion of vehicle is derived by means of this model. The stability of the spacecraft is investigated by using feedback controllers such as optimal feedback control law and Lyapunov-based control law.

Chapter 5 discusses results which are obtained from two different models. Using different physical parameters, the stability of the spacecraft is viewed. This part demonstrates that the thesis makes a verification with some articles, which belongs to Mahmut Reyhanoglu and Jaime Rubio Hervas, using same conditions. Moreover, differently from the literature, an investigation for mass-spring system with four-inner-mass model is discussed.

2. EQUIVALENT MECHANICAL MODELS UNDER EXCITATIONS

For a representation of equivalent mechanical models, first three modes of motion of the fuel tank are demonstrated and figures are compared with Figure 1.1.

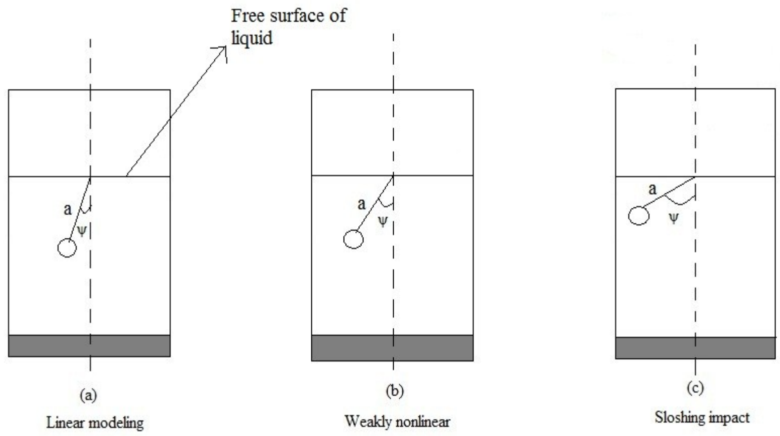

Figure 2.1: First three modes of motion for a simple-pendulum system

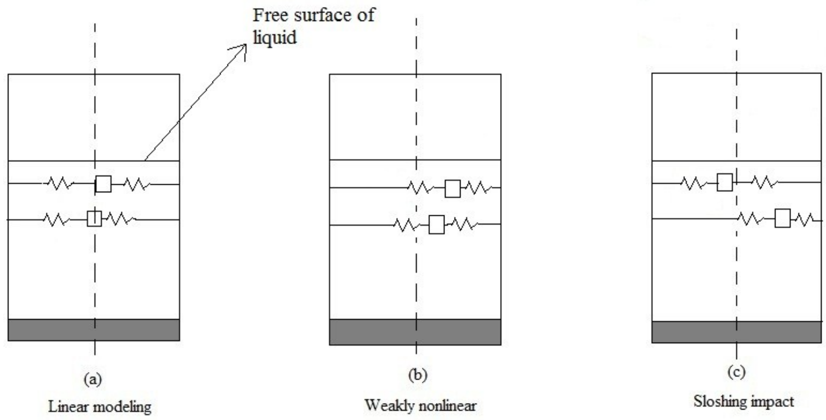

Figure 2.2: First three modes of motion for a mass-spring system

This chapter demonstrates attitudes of the mechanical systems when the models are subjected to lateral and pitching excitations. Force and moment equations are investigated theoretically and compared between each other.

2.1 Multi-Mass-Spring System

General concept in literature is applied to a multi-mass-spring system so as to acquire alike model with a dashpot. For a system in Fig 2.3, in consideration of kinetic energy, potential energy and Rayleigh dissipation function, the equations of motion are derived by means of Lagrange equation.

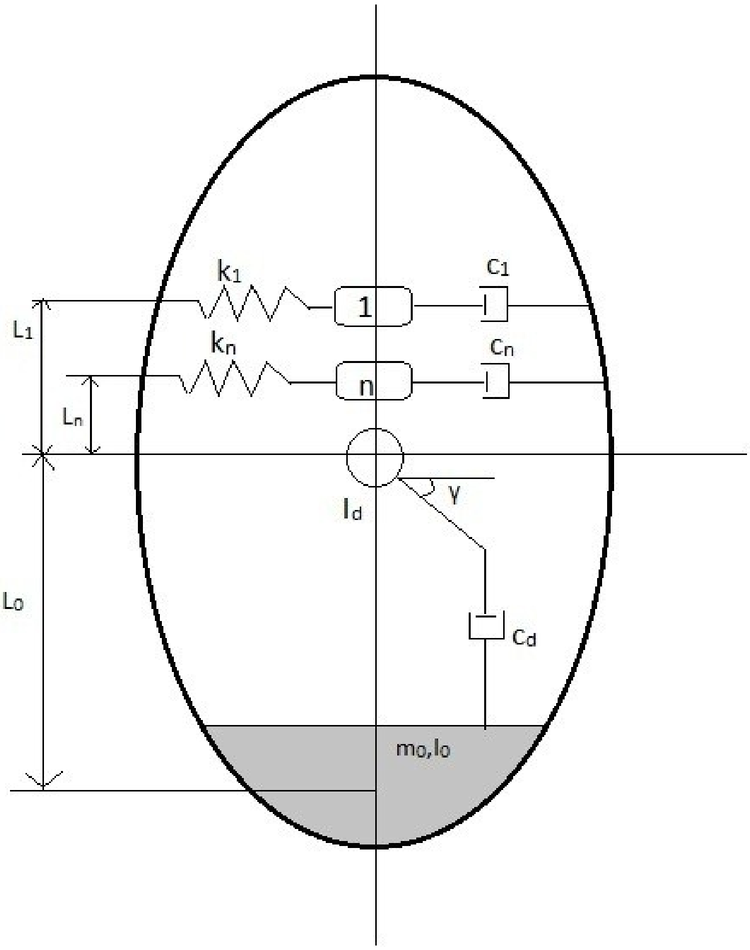

Figure 2.3: Undamped model under excitations for multi-mass-spring system

Total kinetic energy;

$$T = \frac{1}{2}m_0\left(\dot{x} - L_0\dot{\psi}\right)^2 + \frac{1}{2}I_0\dot{\psi}^2 + \frac{1}{2}\sum_{n=1}^{\infty} m_n\left(\dot{s}_n + \dot{x} + L_n\dot{\psi}\right)^2 + \frac{1}{2}I_d\left(\dot{\psi} + \dot{\gamma}\right)^2 \quad \textbf{(2.1)}$$

Potential energy;

$$U = \frac{1}{2} g\psi^2 m_0 L_0 - \frac{1}{2} g\psi^2 \sum_{n=1}^{\infty} m_n L_n - g\psi \sum_{n=1}^{\infty} m_n s_n + \frac{1}{2} \sum_{n=1}^{\infty} k_n {s_n}^2 \tag{2.2}$$

Rayleigh dissipation function;

$$R = \frac{1}{2} \sum_{n=1}^{\infty} c_n {\dot{s_n}}^2 + \frac{1}{2} c_d \dot{\gamma}^2 \tag{2.3}$$

$$\begin{aligned} L = T - U = {} & \frac{1}{2} m_0 \left(\dot{x} - L_0 \dot{\psi}\right)^2 + \frac{1}{2} I_0 \dot{\psi}^2 + \frac{1}{2} \sum_{n=1}^{\infty} m_n \left(\dot{s}_n + \dot{x} + L_n \dot{\psi}\right)^2 \\ & + \frac{1}{2} I_d \left(\dot{\psi} + \dot{\gamma}\right)^2 - \frac{1}{2} g\psi^2 m_0 L_0 + \frac{1}{2} g\psi^2 \sum_{n=1}^{\infty} m_n L_n \\ & + g\psi \sum_{n=1}^{\infty} m_n s_n - \frac{1}{2} \sum_{n=1}^{\infty} k_n {s_n}^2 \end{aligned} \tag{2.4}$$

Lagrange equation;

$$L = \frac{d}{dt}\left(\frac{\partial L}{\partial \dot{q}_i}\right) - \frac{\partial L}{\partial q_i} + \frac{\partial R}{\partial \dot{q}_i} = Q_i$$

The equations of motion are derived applying Lagrange equation with the generalized forces/moments Q_i and internal coordinates $q_i$which are demonstrated below;

$$q_i = \{x, s_n, \psi, \gamma\}^T \qquad\qquad Q_i = \{-F_x, 0, M_y, 0\}^T$$

Applying Lagrange by using above equations, force, slosh, moment and disc equations are found, respectively;

$$m_0\left(\ddot{x} - L_0 \ddot{\psi}\right) + \sum_{n=1}^{\infty} m_n \left(\ddot{s}_n + \ddot{x} + L_n \ddot{\psi}\right) = -F_x \tag{2.5}$$

$$m_n\left(\ddot{s}_n + \ddot{x} + L_n \ddot{\psi}\right) + k_n s_n + c_n \dot{s}_n - m_n g\psi = 0 \tag{2.6}$$

$$I_0\ddot{\psi} + m_0L_0(\ddot{x} - L_0\ddot{\psi}) - g\sum_{n=1}^{\infty} m_n s_n + \sum_{n=1}^{\infty} m_n L_n\,(\ddot{s}_n + \ddot{x} + L_n\ddot{\psi}) + I_d(\ddot{\psi} + \ddot{\gamma}) = M_y \qquad \textbf{(2.7)}$$

$$I_d(\ddot{\psi} + \ddot{\gamma}) + c_d\dot{\gamma} = 0 \qquad \textbf{(2.8)}$$

2.1.1 Lateral excitation for undamped models

Slosh equation is solved in order to determine the steady-state solution for a multi-mass-spring system under a translational excitation $x(t) = X_0 sin\Omega t$. $\psi = \gamma = 0$ and damping is assumed as zero.

$$m_n(\ddot{x} + \ddot{s}_n) + k_n s_n = 0 \qquad \textbf{(2.9)}$$

$$m_n\ddot{s}_n + k_n s_n = \Omega^2 m_n X_0 sin\Omega t$$

The steady-state solution;

$$s_n = m_n X_0 \frac{\Omega^2}{\omega^2 - \Omega^2} sin\Omega t \qquad \textbf{(2.10)}$$

This solution is utilized so as to derive force and moment equations;

$$-F_x = m_0\ddot{x} + \sum_{n=1}^{\infty} m_n\,(\ddot{s}_n + \ddot{x}) \qquad \textbf{(2.11)}$$

$$F_x = \Omega^2 X_0 sin\Omega t\left[\left(m_0 + \sum_{n=1}^{\infty} m_n\right) + \left(\sum_{n=1}^{\infty} m_n \frac{\Omega^2}{\omega^2 - \Omega^2}\right)\right] \qquad \textbf{(2.12)}$$

$$M_y = m_0L_0\ddot{x} - g\sum_{n=1}^{\infty} m_n s_n + \sum_{n=1}^{\infty} m_n L_n\,(\ddot{s}_n + \ddot{x}) \qquad \textbf{(2.13)}$$

$$M_y = -\Omega^2 X_0 sin\Omega t \left[m_0 L_0 + \sum_{n=1}^{\infty} m_n \left(s_n + \frac{g}{{\omega_n}^2} \right) + \sum_{n=1}^{\infty} m_n \left(s_n + \frac{g}{{\omega_n}^2} \right) \left(\frac{\Omega^2}{\omega^2 - \Omega^2} \right) \right] \quad \textbf{(2.14)}$$

2.1.2 Pitching excitation for undamped models

To get the steady-state solution of slosh equation for a multi-mass-spring system, same steps are applied to the system with a pitching excitation $\psi = \psi_0 sin\Omega t$. It is assumed that damping is zero and the displacement of container is neglected.

$$m_n(\ddot{s}_n + L_n\ddot{\psi}) + k_n s_n - m_n g\psi = 0 \quad \textbf{(2.15)}$$

$$m_n\ddot{s}_n + k_n s_n = m_n(\Omega^2 L_n + g)\psi_0 sin\Omega t$$

The steady-state solution;

$$s_n = \frac{\Omega^2 L_n + g}{{\omega_n}^2 - \Omega^2} \quad \textbf{(2.16)}$$

Force and moment equations are derived by means of the steady-state solution;

$$-F_x = m_0 L_0 \ddot{\psi} + \sum_{n=1}^{\infty} m_n\,(\ddot{s}_n + L_n\ddot{\psi}) \quad \textbf{(2.17)}$$

$$F_x = \psi_0 \Omega^2 sin\Omega t \left[m_0 L_0 + \sum_{n=1}^{\infty} m_n\,(L_n\Omega^2 + g) \left(\frac{{\omega_n}^2}{{\omega_n}^2 - \Omega^2} \right) \right] \quad \textbf{(2.18)}$$

$$M_y = I_0\ddot{\psi} + m_0 {L_0}^2 \ddot{\psi} - g \sum_{n=1}^{\infty} m_n s_n + \sum_{n=1}^{\infty} m_n L_n\,(\ddot{s}_n + L_n\ddot{\psi}) \quad \textbf{(2.19)}$$

$$M_y = \psi_0 \Omega^2 sin\Omega t \left[I_0 + m_0 {L_0}^2 + \sum_{n=1}^{\infty} m_n (L_n \Omega^2 + g)^2 \left(\frac{{\omega_n}^2}{{\omega_n}^2 - \Omega^2} \right) \right] \tag{2.20}$$

2.2 Multi-Pendulum Model

System in Fig. 2.2 is inspired from the models in the literature. Using the expressions of kinetic energy, and potential energy, the equations of motion is derived for the model.

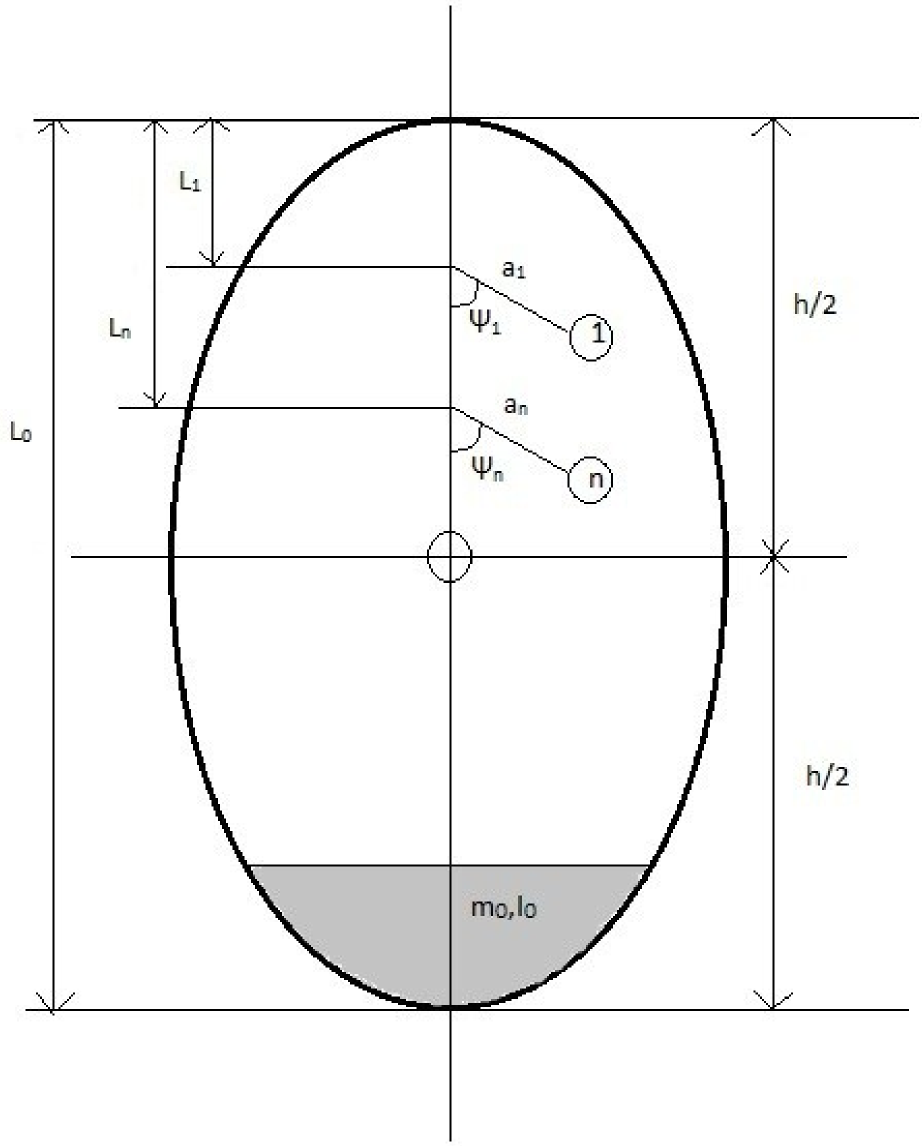

Figure 2.4: A model under excitations for multi-simple-pendulum system

The total kinetic energy;

$$T = \frac{1}{2}m_0\left[\dot{x} + \left(\frac{h}{2} - L_0\right)\dot{\psi}\right]^2 + \frac{1}{2}I_0\dot{\psi}^2 + \frac{1}{2}\sum_{n=1}^{\infty} m_n\left[\left(\frac{h}{2} - L_n - a_n\right)\dot{\psi} + a_n\dot{\psi}_n + \dot{x}\right]^2 \quad \textbf{(2.21)}$$

The total potential energy;

$$U = -m_0 g L_0 cos\psi - \sum_{n=1}^{\infty} m_n\, g[L_n cos\psi + a_n\cos(\psi + \psi_n)] \quad \textbf{(2.22)}$$

Lagrangian form;

$$L = T - U = \frac{1}{2}m_0\left[\dot{x} + \left(\frac{h}{2} - L_0\right)\dot{\psi}\right]^2 + \frac{1}{2}I_0\dot{\psi}^2 + \frac{1}{2}\sum_{n=1}^{\infty} m_n\left[\left(\frac{h}{2} - L_n - a_n\right)\dot{\psi} + a_n\dot{\psi}_n + \dot{x}\right]^2 + m_0 g L_0 cos\psi + \sum_{n=1}^{\infty} m_n\, g[L_n cos\psi + a_n\cos(\psi + \psi_n)] \quad \textbf{(2.23)}$$

Lagrange equation;

$$L = \frac{d}{dt}\left(\frac{\partial L}{\partial \dot{q}_i}\right) - \frac{\partial L}{\partial q_i} + \frac{\partial R}{\partial \dot{q}_i} = Q_i$$

The equations of motion are derived applying Lagrange equation with the generalized forces/moments Q_i and internal coordinates q_i which are demonstrated below;

$$q_i = \{x, \psi, \psi_n\}^T \qquad\qquad Q_i = \{-F_x, M_y, 0\}^T$$

Applying Lagrange by using above equations by means of generalized forces and coordinates, force,moment and slosh equations are found, respectively;

$$-F_x = m_0\left[\ddot{x} + \left(\frac{h}{2} - L_0\right)\ddot{\psi}\right] + \sum_{n=1}^{\infty} m_n\left[\left(\frac{h}{2} - L_n - a_n\right)\ddot{\psi} + a_n\ddot{\psi}_n + \ddot{x}\right] \quad \textbf{(2.24)}$$

$$M_y = m_0\left[\ddot{x} + \left(\frac{h}{2} - L_0\right)\ddot{\psi}\right]\left(\frac{h}{2} - L_0\right) + I_0\ddot{\psi} + \sum_{n=1}^{\infty} m_n a_n\left[\left(\frac{h}{2} - L_n - a_n\right)\ddot{\psi} + a_n\ddot{\psi}_n + \ddot{x}\right] + \sum_{n=1}^{\infty} g m_n[L_n\psi + a_n(\psi + \psi_n)] \tag{2.25}$$

$$\sum_{n=1}^{\infty} m_n\, a_n\left[\left(\frac{h}{2} - L_n - a_n\right)\ddot{\psi} + a_n\ddot{\psi}_n + \ddot{x}\right] + \sum_{n=1}^{\infty} g m_n a_n(\psi + \psi_n) = 0 \tag{2.26}$$

2.2.1 Lateral excitation

Slosh equation is solved so as to determine the steady-state solution for the system under a translational excitation $x(t) = X_0 sin\Omega t$. It is assumed that ψ=0 and the slosh equation becomes;

$$\sum_{n=1}^{\infty} m_n a_n\left(a_n\ddot{\psi}_n + \ddot{x}\right) + \sum_{n=1}^{\infty} g m_n a_n \psi_n = 0 \tag{2.27}$$

$$\sum_{n=1}^{\infty} m_n {a_n}^2\,\ddot{\psi}_n + \sum_{n=1}^{\infty} m_n a_n\, g\psi_n = \Omega^2 X_0 sin\Omega t \sum_{n=1}^{\infty} m_n a_n$$

The steady-state solution;

$$\psi_n = \left[\frac{\Omega^2}{{\omega_n}^2 - \Omega^2}\right]\frac{X_0}{a_n} sin\Omega t \tag{2.28}$$

The solution is utilized so as to derive force and moment equations;

$$-F_x = m_0\ddot{x} + \sum_{n=1}^{\infty} m_n(a_n\ddot{\psi}_n + \ddot{x}) \tag{2.29}$$

$$F_x = m_f X_o \Omega^2 sin\Omega t\left(1 + \sum_{n=1}^{\infty}\frac{m_n}{m_f}\frac{\Omega^2}{{\omega_n}^2 - \Omega^2}\right) \tag{2.30}$$

$$M_y = m_0\ddot{x}\left(\frac{h}{2} - L_0\right) + \sum_{n=1}^{\infty} m_n a_n \left(a_n\ddot{\psi}_n + \ddot{x}\right) + \sum_{n=1}^{\infty} g m_n a_n \psi_n \tag{2.31}$$

$$M_y = -X_o\Omega^2 sin\Omega t\left[m_0\left(\frac{h}{2} - L_0\right) + \sum_{n=1}^{\infty} m_n a_n + \sum_{n=1}^{\infty} m_n\left(a_n - \frac{g}{\Omega^2}\right)\left(\frac{\Omega^2}{\omega_n{}^2 - \Omega^2}\right)\right] \tag{2.32}$$

2.2.2 Pitching excitation

To get the steady-state solution of slosh equation for multi-pendulum-system, same steps are applied to the model with a pitching excitation $\psi = \psi_0 sin\Omega t$ by neglecting the displacement of container.

$$\sum_{n=1}^{\infty} m_n a_n\left[\left(\frac{h}{2} - L_n - a_n\right)\ddot{\psi} + a_n\ddot{\psi}_n\right] + \sum_{n=1}^{\infty} g m_n a_n\left(\psi + \psi_n\right) = 0 \tag{2.33}$$

$$\sum_{n=1}^{\infty} m_n a_n{}^2\,\ddot{\psi}_n + \sum_{n=1}^{\infty} g m_n a_n \psi_n = \psi_0 sin\Omega t\sum_{n=1}^{\infty} m_n a_n\left(\frac{h}{2} - L_n - a_n - g\right)$$

The steady-state solution;

$$\psi_n = \frac{\psi_0 sin\Omega t}{\omega_n{}^2 - \Omega^2}\left(\frac{{}^{h}\!/_{2} - L_n - a_n}{a_n}\Omega^2 - \omega_n{}^2\right) \tag{2.34}$$

Using steady-state solution, force and moment equations are derived;

$$-F_x = m_0\left(\frac{h}{2} - L_0\right)\ddot{\psi} + \sum_{n=1}^{\infty} m_n\left[\left(\frac{h}{2} - L_n - a_n\right)\ddot{\psi} + a_n\ddot{\psi}_n\right] \tag{2.35}$$

$$F_x = \Omega^2 \psi_0 sin\Omega t \left[m_0 L_0 + \sum_{n=1}^{\infty} m_n \left(\frac{h}{2} - L_n - a_n\right) + \sum_{n=1}^{\infty} m_n a_n \left(\frac{h/2 - L_n - a_n}{a_n} - \frac{{\omega_n}^2}{\Omega^2} \right) \frac{\Omega^2}{{\omega_n}^2 - \Omega^2} \right] \tag{2.36}$$

$$M_y = m_0 \left(\frac{h}{2} - L_0\right)^2 \ddot{\psi} + I_0 \ddot{\psi} + \sum_{n=1}^{\infty} m_n a_n \left[\left(\frac{h}{2} - L_n - a_n\right) \ddot{\psi} + a_n \ddot{\psi}_n \right] + \sum_{n=1}^{\infty} g m_n \left(L_n \psi + a_n(\psi + \psi_n)\right) \tag{2.37}$$

$$M_y = -\Omega^2 \psi_0 sin\Omega t \left[m_0 \left(\frac{h}{2} - L_0\right)^2 + I_0 + \sum_{n=1}^{\infty} m_n a_n \left(\frac{h}{2} - L_n - a_n\right) + m_n {a_n}^2 \left(\frac{h/2 - L_n - a_n}{a_n} - \frac{{\omega_n}^2}{\Omega^2} \right) \frac{\Omega^2}{{\omega_n}^2 - \Omega^2} - m_0 g \frac{L_0}{\Omega^2} - \sum_{n=1}^{\infty} m_n a_n (L_n + a_n) \frac{{\omega_n}^2}{\Omega^2} \right] \tag{2.38}$$

3. MASS-SPRING SYSTEM

In this part of study, a multi-mass-spring model is used to design an equivalent mechanical model. The dynamics of a spacecraft with a single propellant tank is investigated by means of this model which is a tool in order to see the stability of vehicle. Spacecraft and internal masses are considered as main rigid body and sub-rigid bodies, respectively. The base body translational velocity vector is denoted by v, the base body angular velocity vector by w, and the vector of internal coordinates by η. The generalized forces and moments over the spacecraft are denoted by τt and τr. Subscript t represents the generalized forces and the subscript r represents the generalized torques that act on the spacecraft. The derivation of the equation of motion, which is under the axial and lateral acceleration is obtained from placing the generalized coordinates, forces and moments into the Lagrange equations. In these equations, L is the Lagrangian form and R is Rayleigh dissipation function [14].

$$\frac{d}{dt}\frac{\partial L}{\partial \mathbf{v}}+\hat{\boldsymbol{\omega}}\frac{\partial L}{\partial \mathbf{v}}=\boldsymbol{\tau}_{\mathbf{t}} \tag{3.1}$$

$$\frac{d}{dt}\frac{\partial L}{\partial \boldsymbol{\omega}}+\hat{\boldsymbol{\omega}}\frac{\partial L}{\partial \boldsymbol{\omega}}+\hat{\mathbf{v}}\frac{\partial L}{\partial \mathbf{v}}=\boldsymbol{\tau}_{\mathrm{r}} \tag{3.2}$$

$$\frac{d}{dt}\frac{\partial L}{\partial \dot{\boldsymbol{\eta}}}-\frac{\partial L}{\partial \boldsymbol{\eta}}+\frac{\partial R}{\partial \dot{\boldsymbol{\eta}}}=0 \tag{3.3}$$

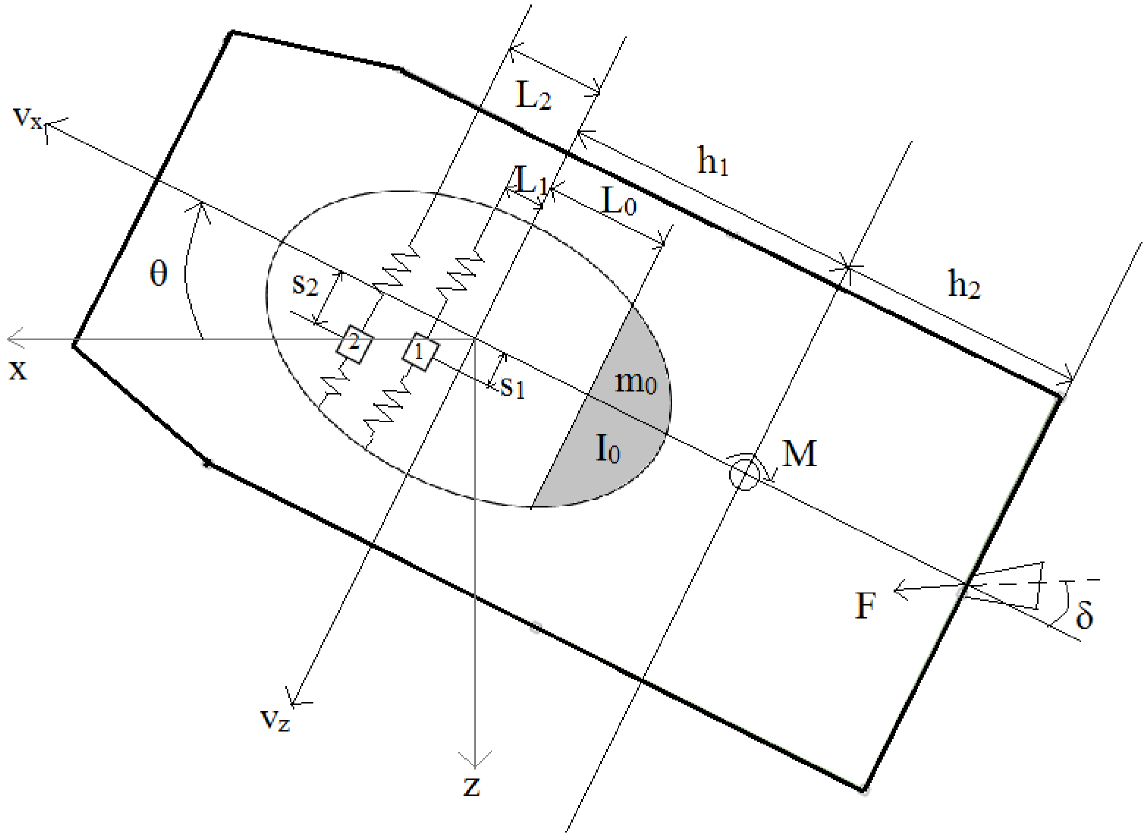

Figure 3.1: Mass-spring system for a spacecraft

As seen in the figure, v_x and v_z are the axial and transverse components of the velocity of the center of tank and θ is the attitude angle of the spacecraft. m_0 is a rigidly attached mass and I_0 is the moment of inertia of this mass, the rest of the propellant is represented as point masses m_n, and their positions from the equilibrium positions are showed by s_n. L_0 and L_n are the locations for masses, h_1 is the distance between the center of the tank and the center of mass of the spacecraft, h_2 is the distance from the thruster to the center of mass of spacecraft. The spacecraft mass m and moment of inertia I, the fuel masses m_0 and m_n, the distances h_1 and h_2 are the constants for this spacecraft. In addition to this, the shape of the tank revises the parameters m_n, h_n and k_n.

The sum of all the masses is equal to the liquid mass and the center of mass of the equivalent mechanical model must have the same height with the liquid mass [15].

$$m_f = m_0 + \sum_{n=1}^{N} m_n \tag{3.4}$$

$$m_0 L_o - \sum_{n=1}^{N} m_n L_n = 0 \qquad \textbf{(3.5)}$$

The position vector of the center of mass m, the position vector of the fuel masses m_0 and m_n, respectively;

$$\vec{r} = (x-h_1)\hat{\imath}+z\hat{k} \qquad \textbf{(3.6)}$$

$$\vec{r}_0=(x+L_0)\hat{\imath}+z\hat{k} \qquad \textbf{(3.7)}$$

$$\vec{r}_n=(x+L_n)\hat{\imath}+(z+s_n)\hat{k} \qquad \textbf{(3.8)}$$

Time derivative of these position vectors;

$$\dot{\vec{r}}=\left(\dot{x}+z\dot{\theta}\right)\hat{\imath}+\left(\dot{z}+(b-x)\dot{\theta}\right)\hat{k} \qquad \textbf{(3.9)}$$

$$\dot{\vec{r}_0}=\left(\dot{x}+z\dot{\theta}\right)\hat{\imath}+\left(\dot{z}-(x+h_0)\dot{\theta}\right)\hat{k} \qquad \textbf{(3.10)}$$

$$\dot{\vec{r}_n}=\left(\dot{x}+(z+s_n)\dot{\theta}\right)\hat{\imath}+\left(\dot{z}-(x+h_n)\dot{\theta}+\dot{s}_n\right)\hat{k} \qquad \textbf{(3.11)}$$

The total kinetic energy;

$$T=\frac{1}{2}m\dot{\vec{r}}^2+\frac{1}{2}m_0\dot{\vec{r}_0}^2+\frac{1}{2}\sum_{n=1}^{N}\left(m_n\dot{\vec{r}_n}^2+I_n\dot{\theta}^2\right)+\frac{1}{2}(I+I_0)\dot{\theta}^2 \qquad \textbf{(3.12)}$$

The total potential energy excluding the gravitational effects;

$$U=\frac{1}{2}\sum_{n=1}^{N}k_n s_n^2 \qquad \textbf{(3.13)}$$

By using above equations the Lagrangian form;

$$\begin{aligned} L = T - U &= \frac{1}{2}m\left[v_x^2 + \left(v_z + b\dot{\theta}\right)^2\right] + \frac{1}{2}m_0\left[v_x^2 + \left(v_z - h_0\dot{\theta}\right)^2\right] \\ &+ \frac{1}{2}(I + I_0)\dot{\theta}^2 \\ &+ \frac{1}{2}\sum_{n=1}^{N} m_n[\left(v_x + s_n\dot{\theta}\right)^2 + (v_z - h_n\dot{\theta} + \dot{s}_n)^2] \\ &+ \frac{1}{2}\sum_{n=1}^{N}\left(I_n\dot{\theta}^2 - k_n s_n^2\right) \end{aligned} \tag{3.14}$$

where $v_x=\dot{x}+z\dot{\theta}$ and $v_z=\dot{z}-x\dot{\theta}$. Rayleigh dissipation function;

$$R=\frac{1}{2}\sum_{n=1}^{N} c_n\dot{s}_n^2 \tag{3.15}$$

The equations of motion are derived applying Lagrange equations with the generalized forces/moments and internal coordinates which are demonstrated below;

$$\eta = \begin{bmatrix} s_1 \\ \vdots \\ s_n \end{bmatrix} \qquad v = \begin{bmatrix} v_x \\ 0 \\ v_z \end{bmatrix} \qquad \omega = \begin{bmatrix} 0 \\ \dot{\theta} \\ 0 \end{bmatrix} \qquad \tau_t = \begin{bmatrix} Fcos\delta \\ 0 \\ Fsin\delta \end{bmatrix} \qquad \tau_r = \begin{bmatrix} 0 \\ M + F(h_1 + h_2)sin\delta \\ 0 \end{bmatrix}$$

$$(m+m_f)a_x+mh_1\dot{\theta}^2+\sum_{n=1}^{N} m_n\left(s_n\ddot{\theta}+2\dot{s}_n\dot{\theta}\right)=F\cos\delta \tag{3.16}$$

$$(m+m_f)a_z+mh_1\ddot{\theta}+\sum_{n=1}^{N} m_n\left(\ddot{s}_n-s_n\dot{\theta}^2\right)=F\sin\delta \tag{3.17}$$

$$I_T\ddot{\theta}+\sum_{n=1}^{N} m_n\left(s_na_x-L_n\ddot{s}_n+2s_n\dot{s}_n\dot{\theta}\right)+mh_1a_z=M+F(h_1+h_2)\sin\delta \tag{3.18}$$

$$m_n\left(\ddot{s}_n+a_z-L_n\ddot{\theta}-s_n\dot{\theta}^2\right)+k_ns_n+c_n\dot{s}_n=0 \tag{3.19}$$

where $a_x=\dot{v}_x+\dot{\theta}v_z$ and $a_z=\dot{v}_z-\dot{\theta}v_x$.

$$I_T = I + I_0 + m h_1{}^2 + m_0 L_0{}^2 + \sum_{n=1}^{N} \left[m_n \left(L_n^2 + s_n^2 \right) + I_n \right]$$

F represents thrust force, *M* is the pitching moment and *δ* is the gimbal deflection angle. Initially, when the fuel burn time is zero, $\dot{\theta}=0$, $s_n=0$, $\dot{s}_n=0$, thrust force *F* is accepted as constant and if the gimbal deflection angle and the pitching moment are zero. Considering these conditions, Eq. (3.16) gives the axial acceleration;

$$a_x = \frac{F}{(m+m_f)} = \dot{v}_x + \dot{\theta} v_z \tag{3.20}$$

$$(m+m_f)\left(\dot{v}_z - \dot{\theta} v_x\right) + m h_1 \ddot{\theta} + \sum_{n=1}^{N} m_n \left(\ddot{s}_n - s_n \dot{\theta}^2 \right) = F \sin\delta \tag{3.21}$$

$$I_T \ddot{\theta} + \sum_{n=1}^{N} m_n (a_x s_n - L_n \ddot{s}_n + 2 s_n \dot{s}_n \dot{\theta}) + m h_1 \left(\dot{v}_z - \dot{\theta} v_x\right) = M + F(h_1+h_2)\sin\delta \tag{3.22}$$

$$\ddot{s}_n + \dot{v}_z - \dot{\theta} v_x - L_n \ddot{\theta} - s_n \dot{\theta}^2 + \frac{k_n}{m_n} s_n + \frac{c_n}{m_n} \dot{s}_n = 0 \tag{3.23}$$

In view of assuming small vehicle motions, the linearized equations of system are obtained;

$$(m+m_f)\left(\dot{v}_z - \dot{\theta} v_x\right) + m h_1 \ddot{\theta} + \sum_{n=1}^{N} m_n \ddot{s}_n = F\delta \tag{3.24}$$

$$I_T \ddot{\theta} + \sum_{n=1}^{N} m_n (a_x s_n - L_n \ddot{s}_n) + m h_1 \left(\dot{v}_z - \dot{\theta} v_x\right) = M + F(h_1+h_2)\delta \tag{3.25}$$

$$\ddot{s}_n + \dot{v}_z - \dot{\theta} v_x - L_n \ddot{\theta} + \frac{k_n}{m_n} s_n + \frac{c_n}{m_n} \dot{s}_n = 0 \tag{3.25}$$

Eliminating $\ddot{s}_n$ in Eqs. (3.21) and (3.22) using Eq. (3.23);

$$(m+m_0)\left(\dot{v}_z-\dot{\theta}v_x\right)+(mh_1-m_0L_0)\ddot{\theta}-\sum_{n=1}^{N}(k_ns_n+c_n\dot{s}_n)=F\sin\delta \tag{3.26}$$

$$(mh_1-m_0L_0)\left(\dot{v}_z-\dot{\theta}v_x\right)+\left(I_T-\sum_{n=1}^{N}m_nL_n^2\right)\ddot{\theta}+N\left(s_i,\dot{s}_i,\dot{\theta}\right)=M+F(h_1+h_2)\sin\delta \tag{3.27}$$

$$N\left(s_i,\dot{s}_i,\dot{\theta}\right)=\sum_{n=1}^{N}\left[(m_na_x+k_nL_n)s_n+L_nc_n\dot{s}_n+2m_ns_n\dot{s}_n\dot{\theta}-m_nL_ns_n\dot{\theta}^2\right]$$

$\left(\dot{v}_z-\dot{\theta}v_x\right)$ is described as u_1 and $\ddot{\theta}$ is described as u_2 defining control transformations to use new control inputs.

$$\begin{bmatrix}u_1\\u_2\end{bmatrix}=\begin{bmatrix}m+m_0 & mh_1-m_0L_0\\ mh_1-m_0L_0 & I_T-\sum_{n=1}^{N}m_nL_n^2\end{bmatrix}^{-1}\begin{bmatrix}F\sin\delta+\sum_{n=1}^{N}(k_ns_n+c_n\dot{s}_n)\\ M+F(h_1+h_2)\sin\delta-N\end{bmatrix} \tag{3.28}$$

$$\ddot{s}_n=-\frac{k_n}{m_n}s_n-\frac{c_n}{m_n}\dot{s}_n-u_1+L_nu_2+s_n\dot{\theta}^2 \tag{3.29}$$

Using the system with new control inputs u_1 and u_2, the gimbal deflection angle and the pitching moment are obtained for $t\leq t_b$.

$$\delta=\sin^{-1}\left(\frac{(m+m_0)u_1+(mh_1-m_0L_0)u_2-\sum_{n=1}^{N}(k_ns_n+c_n\dot{s}_n)}{F}\right) \tag{3.30}$$

$$M=(mh_1-m_0L_0)u_1+\left(I_T-\sum_{n=1}^{N}m_nL_n^2\right)u_2+N\left(s_i,\dot{s}_i,\dot{\theta}\right)-F(h_1+h_2)\sin\delta \tag{3.31}$$

3.1 Feedback Control Laws

Using AVUM Upper Stage rocket Vega's parameters, a mass-spring system is designed for a detailed development of feedback controllers. By means of this model, feedback control laws, which are optimal feedback control law and Lyapunov-based control law, are investigated whether they enable to show the stability of the spacecraft or not.

3.1.1 Optimal feedback control law

In this part, a control method which is called optimal feedback control is applied and the stability of spacecraft and changes in some parameters are viewed. This method is a mathematical discipline using in both science and engineering with lots of applications. In order to apply to the mass-spring system in a case of just one inner-mass, a special case of optimal controller that is called Linear Quadratic Regulator (LQR) is used and this controller aims minimizing the quadratic cost function.

Considering the system,

$$\dot{x} = Ax + Bu \qquad \textbf{(3.32)}$$

where

$$x = \begin{bmatrix} v_z \\ \dot{v_z} \\ \theta \\ \dot{\theta} \\ s_1 \\ \dot{s_1} \end{bmatrix} \qquad \dot{x} = \begin{bmatrix} \dot{v_z} \\ \ddot{v_z} \\ \dot{\theta} \\ \ddot{\theta} \\ \dot{s_1} \\ \ddot{s_1} \end{bmatrix} \qquad u = \begin{bmatrix} \delta \\ M \end{bmatrix}$$

$$A = \begin{bmatrix} 0 & 1 & 0 & 0 & 0 & 0 \\ 0 & 0 & 0 & 0 & 0 & 0 \\ 0 & 0 & 0 & 1 & 0 & 0 \\ 0 & -\dfrac{(m+m_f)L_1 + mh_1}{\alpha} & 0 & v_x\left(\dfrac{(m+m_f)L_1 + mh_1}{\alpha}\right) & -\dfrac{m_1 a_x}{\alpha} & 0 \\ 0 & 0 & 0 & 0 & 0 & 1 \\ 0 & \dfrac{m^2 {h_1}^2 - I_T(m+m_f)}{m_1 \alpha} & 0 & -v_x \dfrac{m^2 {h_1}^2 - I_T(m+m_f)}{m_1 \alpha} & \dfrac{m h_1 a_x}{\alpha} & 0 \end{bmatrix} \qquad \textbf{(3.33)}$$

$$B = \begin{bmatrix} 0 & 0 \\ 0 & 0 \\ 0 & 0 \\ F\left(\dfrac{L_1 - h_2}{\alpha}\right) & -\dfrac{1}{\alpha} \\ 0 & 0 \\ \dfrac{I_T m - h_2 m {h_1}^2}{m_1 h_1 \alpha} & -\dfrac{m h_1}{m_1 \alpha} \end{bmatrix} \qquad \textbf{(3.34)}$$

$$\alpha = I_T + mh_1L_1$$

Considering to stabilize the system, designing state feedback control,

$$u = -Kx \quad \textbf{(3.35)}$$

To define the cost functional, *K* is designed as tradeoff between the response of the system and the control effort, and u is searched to minimize the index. The cost function,

$$J = \int_0^\infty [x^T(t)Qx(t) + u^T(t)Ru(t)]dt \quad \textbf{(3.36)}$$

Here, Q and R are an n x n symmetric positive-semi definite weighting matrix, and an m x m symmetric positive-definite weighting matrix, respectively.

The optimal control gain matrix *K* is found by solving Riccati equation. The Algebraic Riccati Equation;

$$A^TP + PA + Q - (PB)R^{-1}(B^TP) = 0 \quad \textbf{(3.37)}$$

and the optimal state-feedback matrix gain *K*;

$$K = R^{-1}(B^TP) \quad \textbf{(3.38)}$$

As a hint, MATLAB's LQR command is [K, P, E] = lqr (A, B, Q, R) can be used so as to solve The Algebraic Riccati Equation [16].

3.1.2 Lyapunov-based control law

Lyapunov-based control, which is used to see whether a dynamical system is stable, is chosen to bound the uncertainties for a closed-loop system. Though Lyapunov control method is applied to nonautonomous system $\dot{x} = f(x, t)$s, it can be restrained to time-invariant nonlinear systems $\dot{x} = f(x)$ [17]. Even though this controller is not interested in system's performance, it is a significant tool for nonlinear control system design and stability.

Considering a system $\dot{x} = f(x)$ with a fixed point x*, a continuously differentiable and real valued candidate Lyapunov function is found [18]. Lyapunov method consists of

i. Choosing a positive definite candidate Lyapunov function V(x)
ii. Calculating function's time derivative $\dot{V}(x)$, and checking whether it is negative valued for stability

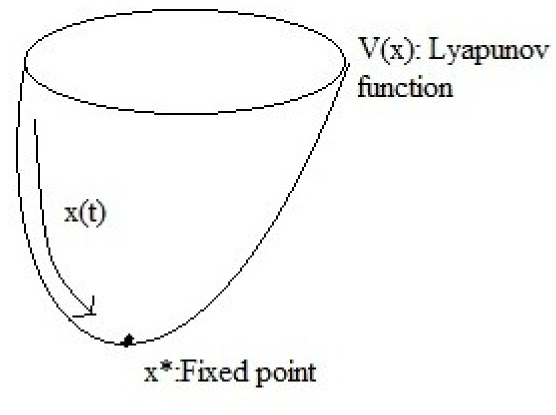

Figure 3.2: The trajectory of Lyapunov function

Constructing Lyapunov functions is not easy and there is no systematic way. An accurate function is found by trial and error and sometimes one can get the function by working backwards [19].

Utilizing the information from the articles and having the inputs from previous chapter, a candidate Lyapunov function V is determined;

$$\dot{v}_z = u_1 + \dot{\theta} v_x(t) \qquad \qquad \ddot{\theta} = u_2$$

$$V = \frac{p_1}{2} {v_z}^2 + \frac{p_2}{2} \theta^2 + \frac{p_3}{2} \dot{\theta}^2 \tag{3.39}$$

The time derivative of function along the trajectories;

$$\dot{V} = p_1 v_z \dot{v}_z + p_2 \theta \dot{\theta} + p_3 \dot{\theta} \ddot{\theta} \tag{3.40}$$

Substituting the control inputs into Eq. (3.36) new form is obtained;

$$\dot{V} = p_1 v_z u_1 + \dot{\theta}(p_1 v_z v_x + p_2\theta + p_3 u_2) \quad \textbf{(3.41)}$$

The feedback laws;

$$u_1 = -M_1 v_z \quad \textbf{(3.42)}$$

$$u_2 = \frac{1}{p_3}\left(p_2\theta + M_2\dot{\theta}\right) \quad \textbf{(3.43)}$$

where p_1, p_2, p_3, M_1 and M_2 are positive constants and the numbers satisfy the conditions for Lyapunov function.

3.2 Simulations

AVUM upper stage spacecraft Vega's parameters, used in this part, are based on an article which belongs to Reyhanoglu and Hervas are utilized in order to make a simulation [7]. In calculations, results are obtained by taking into account slosh modes for two-inner-mass model and four-inner-mass model. Necessary physical parameters are given in Table 3.1 and Table 3.2. Initial conditions for the equivalent mass-spring system, $v_{x_0} = 3000\ m/s$, $v_{z_0} = 150\ m/s$, $\theta_0 = 5°$, $\dot{\theta}_0 = 0°$, $s_{1_0} = 0.15\ m$, $s_{2_0} = -0.15$, $s_{3_0} = 0.075\ m$, $s_{4_0} = -0.075\ m$. In all of these calculations, fuel burn time is assumed 660 s for the simulations [21].

Table 3.1: Physical Parameters for Mass-Spring System with Two-Inner-Mass

Parameter	*Value*	*Parameter*	*Value*
$\boldsymbol{m}$	$975\ kg$	$\boldsymbol{F}$	$2450\ N$
$\boldsymbol{m_0}$	$205\ kg$	$\boldsymbol{I}$	$400\ kgm^2$
$\boldsymbol{m_1}$	$195\ kg$	$\boldsymbol{I_0}$	$44.1\ kgm^2$
$\boldsymbol{m_2}$	$6.5\ kg$	$\boldsymbol{I_1}$	$10\ kgm^2$
$\boldsymbol{k_1}$	$1174\ N/m$	$\boldsymbol{I_2}$	$1\ kgm^2$
$\boldsymbol{k_2}$	$120\ N/m$	$\boldsymbol{c_1}$	$48\ Ns/m$
$\boldsymbol{L_0}$	$0.135\ m$	$\boldsymbol{c_2}$	$2.75\ Ns/m$
$\boldsymbol{L_1}$	$-0.145\ m$	$\boldsymbol{h_1}$	$-0.6\ m$
$\boldsymbol{L_2}$	$0.035\ m$	$\boldsymbol{h_2}$	$1.2\ m$

Table 3.2: Physical Parameters for Mass-Spring System with Four-Inner-Mass

Parameter	*Value*	*Parameter*	*Value*
$\boldsymbol{m}$	$975\ kg$	$\boldsymbol{F}$	$2450\ N$
$\boldsymbol{m_0}$	$205\ kg$	$\boldsymbol{I}$	$400\ kgm^2$
$\boldsymbol{m_1}$	$194\ kg$	$\boldsymbol{I_0}$	$44.1\ kgm^2$
$\boldsymbol{m_2}$	$6\ kg$	$\boldsymbol{I_1}$	$10\ kgm^2$
$\boldsymbol{m_3}$	$1\ kg$	$\boldsymbol{I_2}$	$1\ kgm^2$
$\boldsymbol{m_4}$	$0.5\ kg$	$\boldsymbol{I_3}$	$0.5\ kgm^2$
$\boldsymbol{k_1}$	$1174\ N/m$	$\boldsymbol{I_4}$	$0.1\ kgm^2$
$\boldsymbol{k_2}$	$120\ N/m$	$\boldsymbol{c_1}$	$48\ Ns/m$
$\boldsymbol{k_3}$	$12\ N/m$	$\boldsymbol{c_2}$	$2.75\ Ns/m$
$\boldsymbol{k_4}$	$6\ N/m$	$\boldsymbol{c_3}$	$2\ Ns/m$
$\boldsymbol{L_0}$	$0.135\ m$	$\boldsymbol{c_4}$	$1.5\ Ns/m$
$\boldsymbol{L_1}$	$-0.145\ m$	$\boldsymbol{h_1}$	$-0.6\ m$
$\boldsymbol{L_2}$	$0.035\ m$	$\boldsymbol{h_2}$	$1.2\ m$
$\boldsymbol{L_3}$	$-0.023\ m$	$\boldsymbol{L_4}$	$0.017\ m$

As mentioned before, $(\dot{v}_z\text{-}\dot{\theta}v_x)$ is described as u_1 and $\ddot{\theta}$ is described as u_2 defining control transformations to use new control inputs. Starting from this point of view, to investigate the stability of the spacecraft, u_1 and u_2 are utilized.

3.2.1 Linear quadratic regulator

In section 3.1, Linear Quadratic Regulator is defined as the theory of optimal control for a dynamic system. Physical parameters are substituted in the matrices, which is used for control purpose.

$$A = \begin{bmatrix} 0 & 1 & 0 & 0 & 0 & 0 \\ 0 & 0 & 0 & 0 & 0 & 0 \\ 0 & 0 & 0 & 1 & 0 & 0 \\ 0 & 0.8704 & 0 & -0.8704v_x & -0.3826 & 0 \\ 0 & 0 & 0 & 0 & 0 & 1 \\ 0 & -4.4731 & 0 & 4.4731v_x & -0.2296 & 0 \end{bmatrix}$$

$$B = \begin{bmatrix} 0 & 0 \\ 0 & 0 \\ 0 & 0 \\ -3.6527 & -0.0011 \\ 0 & 0 \\ -7.1777 & 0.0032 \end{bmatrix}$$

The weigthing matrices;

$$Q = \begin{bmatrix} 1 & 0 & 0 & 0 & 0 & 0 \\ 0 & 1 & 0 & 0 & 0 & 0 \\ 0 & 0 & 1 & 0 & 0 & 0 \\ 0 & 0 & 0 & 1 & 0 & 0 \\ 0 & 0 & 0 & 0 & 1 & 0 \\ 0 & 0 & 0 & 0 & 0 & 1 \end{bmatrix}$$

$$R = \begin{bmatrix} 10 & 0 \\ 0 & 0.1 \end{bmatrix}$$

The optimal control gain matrix K cannot be found because of the system's chaotic behavior. Due to the fact that there are time-varying terms in matrix A, the poles of A are not controllable through B.

3.2.2 Lyapunov-based controller

Specified parameters are substituted into Lyapunov function for mass-spring system and this edited function is utilized to investigate the stability of the spacecraft.

Table 3.3: Necessary physical parameters of mass-spring system for Lyapunov function

Parameters	Value
p_1	8*10^{-7}
p_2	2500
p_3	500
M_1	10^4
M_2	10^4

$$V = 4 * 10^{-7} {v_z}^2 + 1250\theta^2 + 250\dot{\theta}^2$$

$$\dot{V} = 8{*}10^{-7} v_z u_1 + \dot{\theta}\left(8{*}10^{-7} v_z v_x + 2500\theta + 500 u_2\right)$$

$$u_1 = -10^4 v_z \qquad u_2 = 5\theta + 20\dot{\theta}$$

The basis conditions for Lyapunov function which are $V > 0$ and $\dot{V} \leq 0$ are theoretically proven.

3.2.3 Simulation results for mass-spring system

3.2.3.1 Graphics for two-inner-mass model

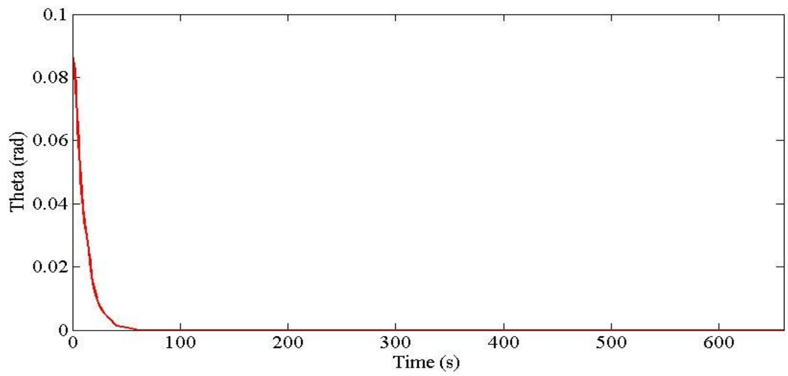

Figure 3.3: Change of the attitude angle with respect to time for two-inner-mass model

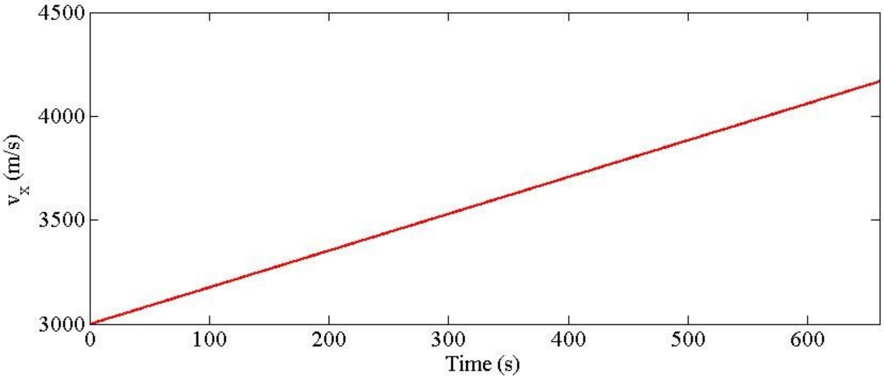

Figure 3.4: Change of the axial component of velocity of spacecraft with respect to time for two-inner-mass model

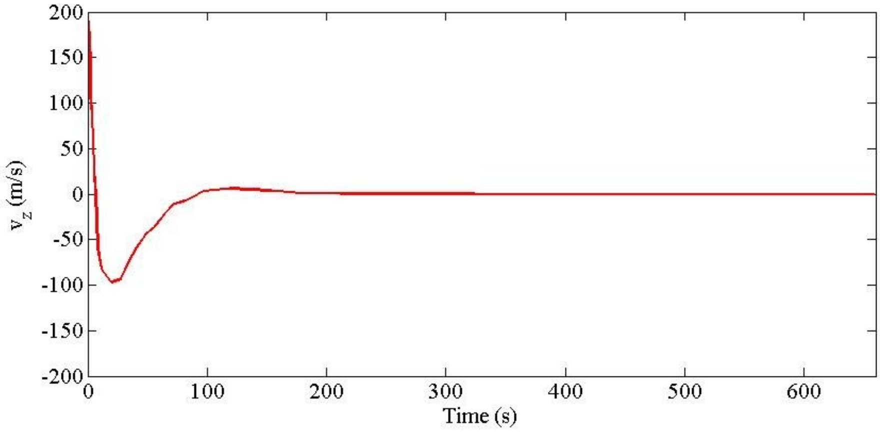

Figure 3.5: Change of the transverse component of velocity of spcacraft with respect to time for two-inner-mass model

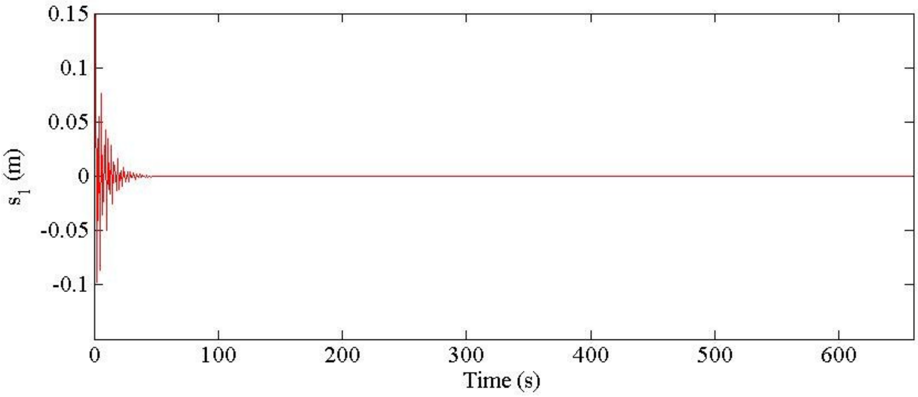

Figure 3.6: Change of s_1 with respect to time for two-inner-mass model

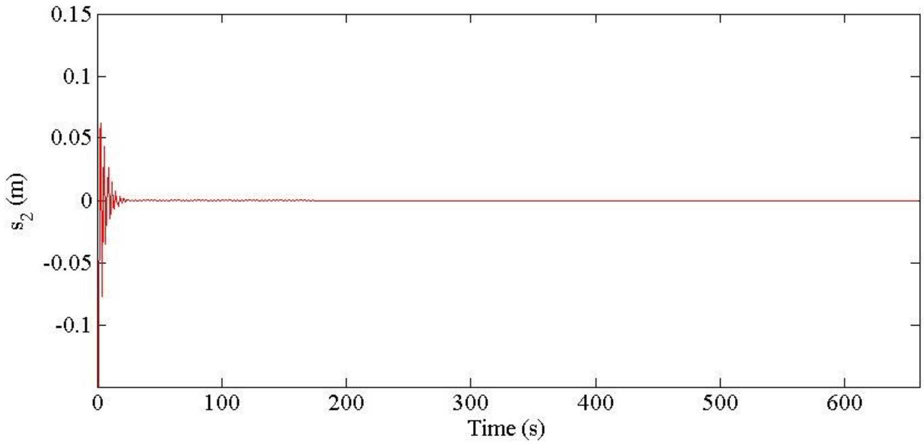

Figure 3.7: Change of s_2 with respect to time for two-inner-mass model

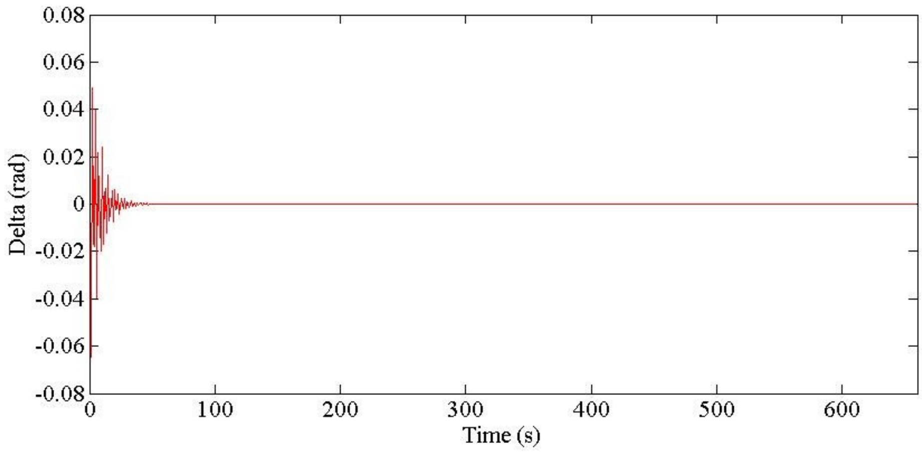

Figure 3.8: Change of gimbal deflection angle δ with respect to time for two-inner-mass model

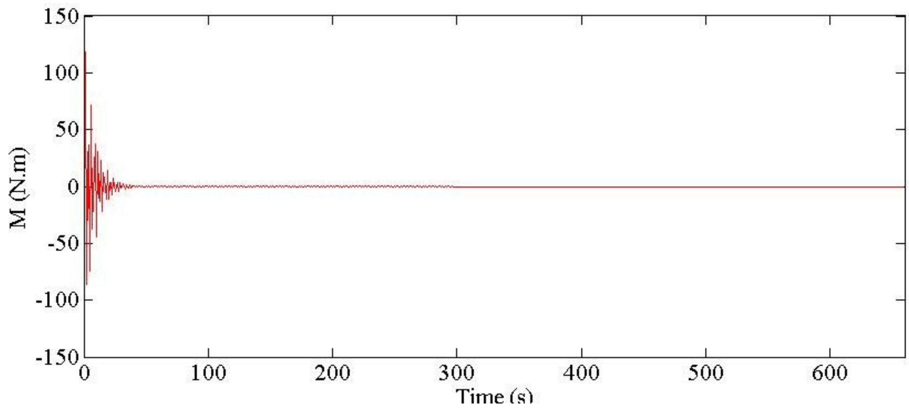

Figure 3.9: Change of pitching moment M with respect to time for two-inner-mass model

3.2.3.2 Graphics for four-inner-mass model

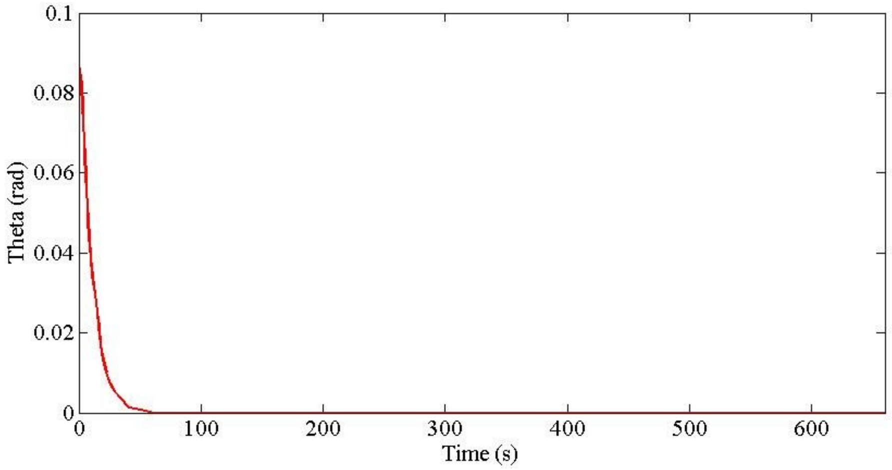

Figure 3.10: Change of the attitude angle with respect to time for four-inner-mass model

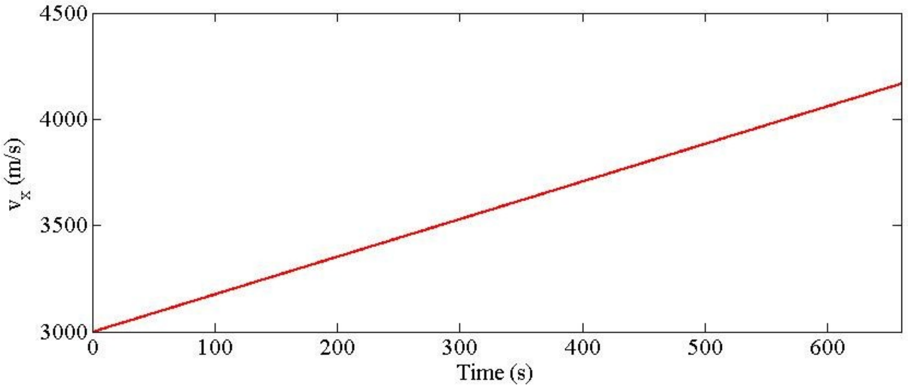

Figure 3.11: Change of the axial component of velocity of spacecraft with respect to time for four-inner-mass model

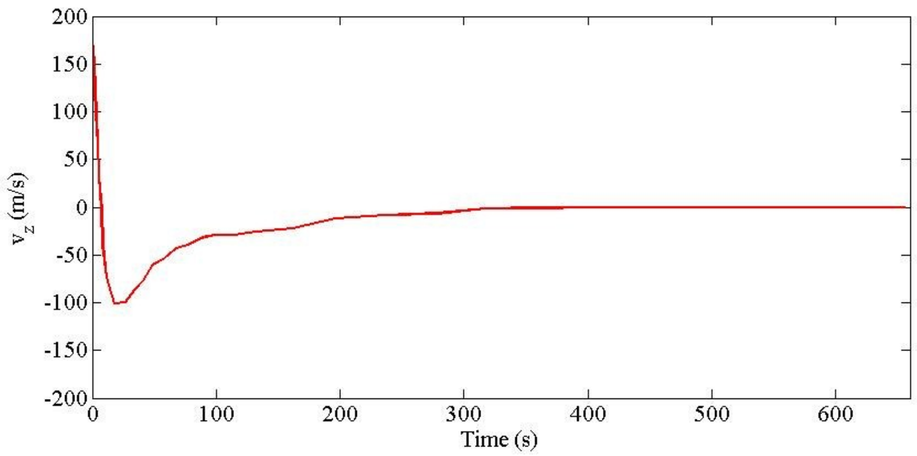

Figure 3.12: Change of the transverse component of velocity of spacecraft with respect to time for four-inner-mass model

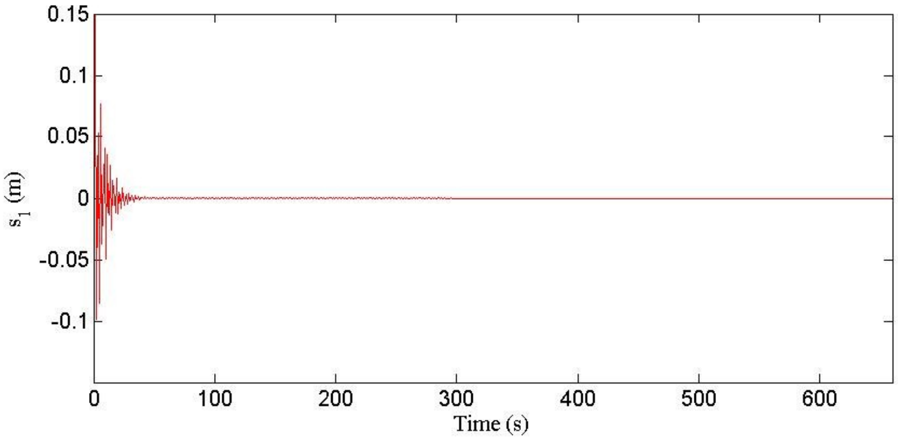

Figure 3.13: Change of s_1 with respect to time for four-inner-mass model

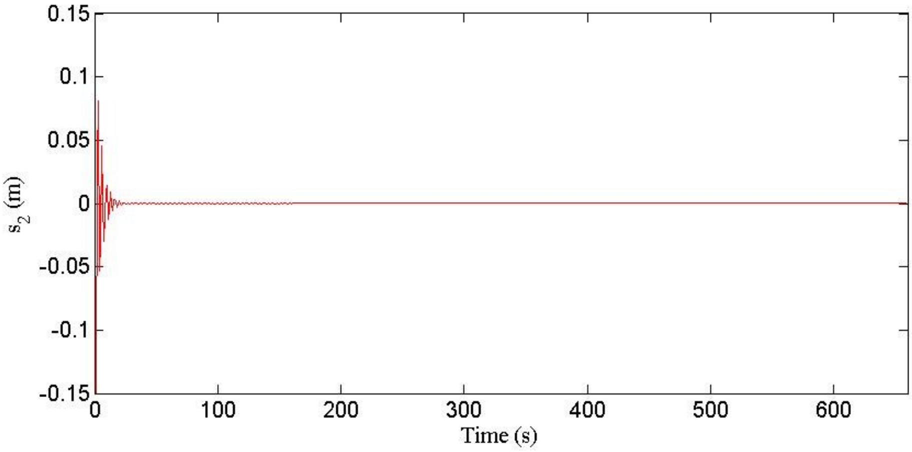

Figure 3.14: Change of s_2 with respect to time for four-inner-mass model

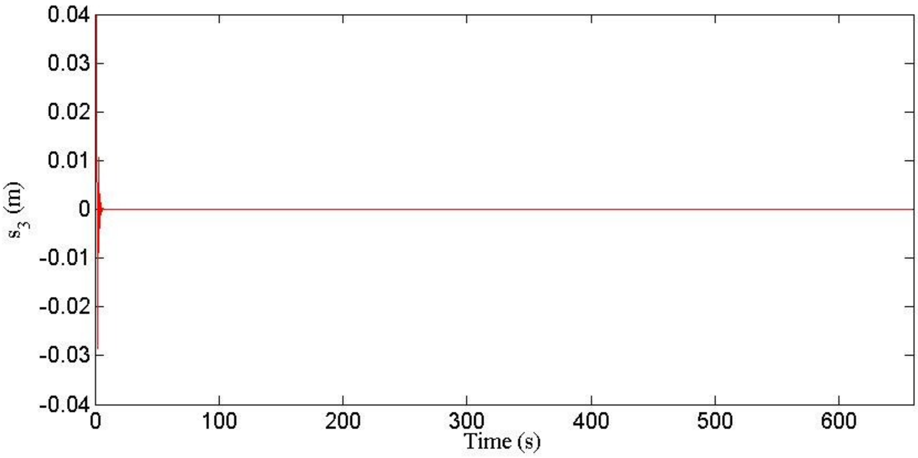

Figure 3.15: Change of s_3 with respect to time for four-inner-mass model

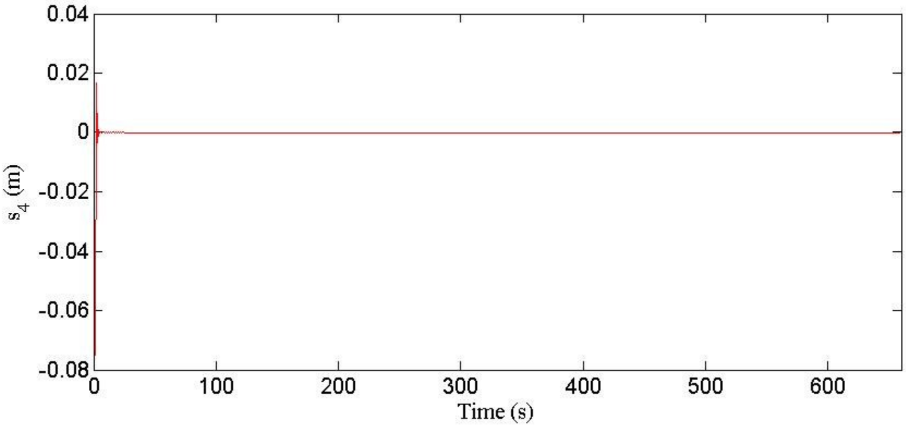

Figure 3.16: Change of s_4 with respect to time for four-inner-mass model

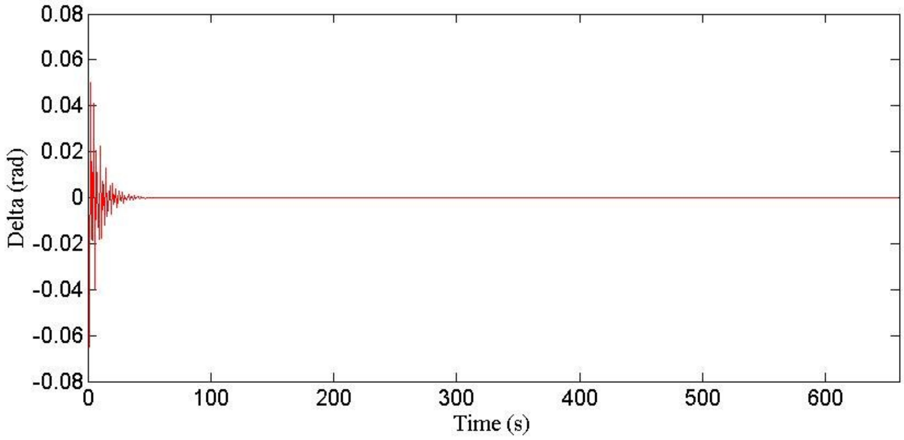

Figure 3.17: Change of gimbal deflection angle δ with respect to time for four-inner-mass model

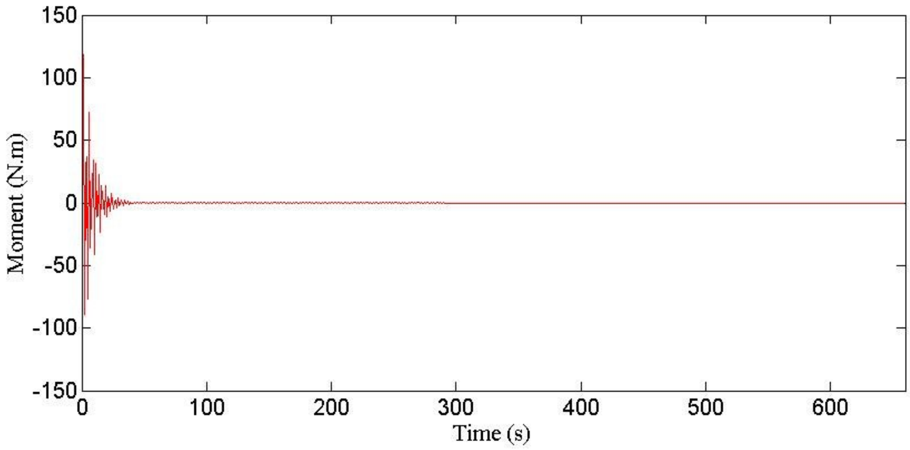

Figure 3.18: Change of pitching moment M with respect to time for four-inner-mass model

4. SIMPLE PENDULUM MODEL

In this chapter of dissertation, a simple pendulum model is used to design an equivalent mechanical model. As mentioned in previous chapter, in order to investigate slosh effect over the stability of spacecraft, liquid fuel can be modeled as mechanical model. Starting from this point of view, a single pendulum is utilized for a space vehicle with a gimbaled thrust engine. Equations of motion is obtained from using Lagrange equations with some parameters, which are mentioned in the previous part. Here, L is Lagrangian form and R is Rayleigh dissipation function.

$$\frac{d}{dt}\frac{\partial L}{\partial \mathbf{v}}+\widehat{\boldsymbol{\omega}}\frac{\partial L}{\partial \mathbf{v}}=\boldsymbol{\tau}_t \tag{4.1}$$

$$\frac{d}{dt}\frac{\partial L}{\partial \boldsymbol{\omega}}+\widehat{\boldsymbol{\omega}}\frac{\partial L}{\partial \boldsymbol{\omega}}+\hat{\mathbf{v}}\frac{\partial L}{\partial \mathbf{v}}=\boldsymbol{\tau}_r \tag{4.2}$$

$$\frac{d}{dt}\frac{\partial L}{\partial \dot{\boldsymbol{\eta}}}-\frac{\partial L}{\partial \boldsymbol{\eta}}+\frac{\partial R}{\partial \dot{\boldsymbol{\eta}}}=0 \tag{4.3}$$

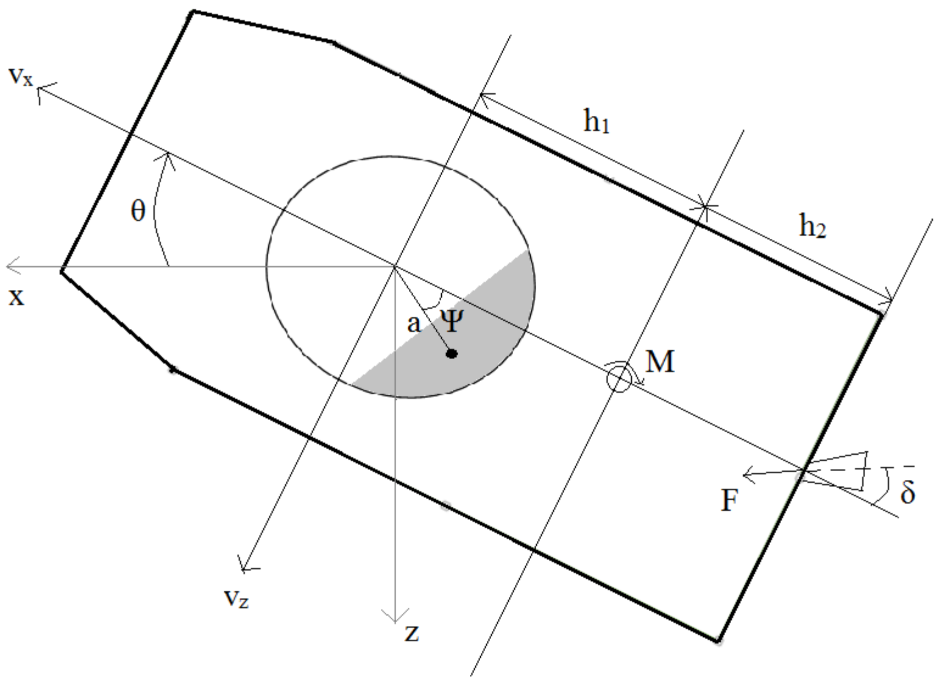

Figure 4.1: Simple-pendulum model for a spacecraft

As seen in the figure, v_x and v_z are the axial and transverse components of the velocity of the center of tank, respectively, θ is the attitude angle of the spacecraft and ψ is the angle of the pendulum. a is the length of pendulum, h_1 is the distance between the center of the tank and the center of mass of the spacecraft, h_2 is the distance from the thruster to the center of mass of spacecraft. m and m_f are the spacecraft mass and the total mass of the liquid fuel, I and I_f are the moment of inertia of spacecraft and liquid fuel seriatim.

The position vector of the center of mass of the spacecraft and the position vector of the fuel, respectively;

$$\vec{r} = (x-h_1)\hat{\imath}+z\hat{k} \tag{4.4}$$

$$\vec{r}_f=(x-a\cos\psi)\hat{\imath}+(z+a\sin\psi)\hat{k} \tag{4.5}$$

Time derivative of these position vectors;

$$\dot{\vec{r}}=\left(\dot{x}+z\dot{\theta}\right)\hat{\imath}+\left(\dot{z}-x\dot{\theta}+h_1\dot{\theta}\right)\hat{k} \tag{4.6}$$

$$\dot{\vec{r}}_f=[\dot{x}+a\dot{\psi}\sin\psi+\dot{\theta}(z+a\sin\psi)]\hat{\imath}+[\dot{z}+a\dot{\psi}\cos\psi-\dot{\theta}(x-a\cos\psi)]\hat{k} \tag{4.7}$$

The total kinetic energy;

$$T=\frac{1}{2}m\dot{\vec{r}}^2+\frac{1}{2}m_f\dot{\vec{r}}_f^{\,2}+\frac{1}{2}I\dot{\theta}^2+\frac{1}{2}I_f(\dot{\theta}+\dot{\psi})^2 \tag{4.8}$$

There is no potential energy because of the fact that gravitational effects are ignored. Therefore, Lagrangian form is equal to total kinetic energy.

$$\begin{aligned} L = T &= \frac{1}{2}m\dot{\vec{r}}^2+\frac{1}{2}m_f\dot{\vec{r}}_f^{\,2}+\frac{1}{2}I\dot{\theta}^2+\frac{1}{2}I_f(\dot{\theta}+\dot{\psi})^2 \\ &= \frac{1}{2}m\left[v_x^2+\left(v_z+h_1\dot{\theta}\right)^2\right] \\ &+\frac{1}{2}m_f\left[(v_x+a\left(\dot{\theta}+\dot{\psi}\right)\sin\psi)^2+(v_z+a\left(\dot{\theta}+\dot{\psi}\right)\cos\psi)^2\right] \\ &+\frac{1}{2}I\dot{\theta}^2+\frac{1}{2}I_f(\dot{\theta}+\dot{\psi})^2 \end{aligned} \tag{4.9}$$

where $v_x=\dot{x}+z\dot{\theta}$ and $v_z=\dot{z}-x\dot{\theta}$. Rayleigh dissipation function;

$$R = \frac{1}{2}\varepsilon\dot{\psi}^2 \tag{4.10}$$

The equations of motion are derived applying Lagrange equations with the generalized forces/moments and internal coordinates which are demonstrated below;

$$\eta = \psi \qquad v = \begin{bmatrix} v_x \\ 0 \\ v_z \end{bmatrix} \quad \omega = \begin{bmatrix} 0 \\ \dot{\theta} \\ 0 \end{bmatrix} \quad \tau_t = \begin{bmatrix} F cos\delta \\ 0 \\ F sin\delta \end{bmatrix} \quad \tau_r = \begin{bmatrix} 0 \\ M + F(h_1 + h_2) sin\delta \\ 0 \end{bmatrix}$$

$$(m + m_f)a_x + m_f a(\ddot{\theta} + \ddot{\psi})\sin\psi + mh_1\dot{\theta}^2 + m_f a\left(\dot{\theta} + \dot{\psi}\right)^2\cos\psi = F\cos\delta \tag{4.11}$$

$$(m + m_f)a_z + m_f a(\ddot{\theta} + \ddot{\psi})\cos\psi + mh_1\ddot{\theta} - m_f a\left(\dot{\theta} + \dot{\psi}\right)^2\sin\psi = F\sin\delta \tag{4.12}$$

$$\left(I + mh_1{}^2\right)\ddot{\theta} + mh_1 a_z - \varepsilon\dot{\psi} = M + F(h_1 + h_2)\sin\delta \tag{4.13}$$

$$(I_f + m_f a^2)\left(\ddot{\theta} + \ddot{\psi}\right) + m_f a[a_x \sin\psi + a_z \cos\psi] + \varepsilon\dot{\psi} = 0 \tag{4.14}$$

where $a_x = \dot{v}_x + \dot{\theta}v_z$ and $a_z = \dot{v}_z - \dot{\theta}v_x$.

F represents thrust force, *M* is the pitching moment and *δ* is the gimbal deflection angle. At first stage, when the fuel burn time is zero, $\dot{\theta}=0$, $\psi = 0$, $\dot{\psi} = 0$, thrust force *F* is accepted as constant and if the gimbal deflection angle and the pitching moment are zero. The linearized equations of system are obtained by assuming small gimbal deflection;

$$(m + m_f)a_x + m_f a(\ddot{\theta} + \ddot{\psi})\sin\psi + mh_1\dot{\theta}^2 + m_f a\left(\dot{\theta} + \dot{\psi}\right)^2\cos\psi = F \tag{4.15}$$

$$(m + m_f)a_z + m_f a(\ddot{\theta} + \ddot{\psi})\cos\psi + mh_1\ddot{\theta} - m_f a\left(\dot{\theta} + \dot{\psi}\right)^2\sin\psi = F\delta \tag{4.16}$$

$$\left(I + mh_1{}^2\right)\ddot{\theta} + mh_1 a_z - \varepsilon\dot{\psi} = M + F(h_1 + h_2)\delta \tag{4.17}$$

$$(I_f + m_f a^2)\left(\ddot{\theta} + \ddot{\psi}\right) + m_f a[a_x \sin\psi + a_z \cos\psi] + \varepsilon\dot{\psi} = 0 \tag{4.18}$$

For a_x and a_z, Eqs. (4.15) and (4.16) are solved to find the accelerations, then these accelerations are eliminated from the other equations.

$$\left[I+\frac{mm_f}{m+m_f}\left({h_1}^2-ah_1\cos\psi\right)\right]\ddot{\theta}-\frac{mm_f}{m+m_f}ah_1\ddot{\psi}\cos\psi \tag{4.19}$$
$$+\frac{mm_f}{m+m_f}ah_1\left(\dot{\theta}+\dot{\psi}\right)^2\sin\psi-\varepsilon\dot{\psi}$$
$$=M+\left(\frac{m_f h_1}{m+m_f}+h_2\right)F\delta$$

$$\left[I_f+\frac{mm_f}{m+m_f}(a^2-ah_1\cos\psi)\right]\ddot{\theta}+\left(I_f+\frac{mm_f}{m+m_f}a^2\right)\ddot{\psi} \tag{4.20}$$
$$+\left(\frac{m_f a}{m+m_f}F-\frac{mm_f}{m+m_f}ah_1\dot{\theta}^2\right)\sin\psi+\varepsilon\dot{\psi}$$
$$=-\frac{m_f a}{m+m_f}F\delta\cos\psi$$

The linearized equations are obtained by assuming small θ, ψ and changes in them;

$$\left[I+\frac{mm_f}{m+m_f}\left({h_1}^2-ah_1\right)\right]\ddot{\theta}-\frac{mm_f}{m+m_f}ah_1\ddot{\psi}-\varepsilon\dot{\psi} \tag{4.21}$$
$$=M+\left(\frac{m_f h_1}{m+m_f}+h_2\right)F\delta$$

$$\left[I_f+\frac{mm_f}{m+m_f}(a^2-ah_1)\right]\ddot{\theta}+\left(I_f+\frac{mm_f}{m+m_f}a^2\right)\ddot{\psi}+\left(\frac{m_f a}{m+m_f}F\right)\sin\psi \tag{4.22}$$
$$+\varepsilon\dot{\psi}=-\frac{m_f a}{m+m_f}F\delta$$

Ultimately, by taking Eqs. (4.12) and (4.13) into consideration, $\left(\dot{v}_z\text{-}\dot{\theta}v_x\right)$ and $\ddot{\theta}$ are described as *u₁* and *u₂*, respectively, defining control transformations to use new control inputs.

$$\begin{bmatrix}u_1\\u_2\end{bmatrix}=\begin{bmatrix}m+m_f & m_f a\cos\psi+mh_1\\ mh_1 & I+m{h_1}^2\end{bmatrix}^{-1}\begin{bmatrix}F\sin\delta\text{-}m_f a\ddot{\psi}\cos\psi+m_f a\left(\dot{\theta}+\dot{\psi}\right)^2\sin\psi\\ M+F(h_1+h_2)\sin\delta+\varepsilon\dot{\psi}\end{bmatrix} \tag{4.23}$$

Using the system with new control inputs u_1 and u_2, the gimbal deflection angle and the pitching moment are obtained for $t\leq t_b$.

$$\delta = \sin^{-1}\left(\frac{(m+m_f)u_1+(m_f a\cos\psi+mh_1)u_2+m_f a\cos\psi\ddot{\psi} - m_f a\left(\dot{\theta}+\dot{\psi}\right)^2 sin\psi}{F}\right) \quad \mathbf{(4.24)}$$

$$M = mh_1u_1 + \left(I + mh_1{}^2\right)u_2 - F(h_1 + h_2)sin\delta - \varepsilon\dot{\psi} \quad \mathbf{(4.25)}$$

The slosh equation is found by regulating Eq. (4.18) and then $\ddot{\psi}$ is eliminated from Eqs. (4.23) and (4.24);

$$\ddot{\psi} = -u_2 - \frac{m_f a}{I_f + m_f a^2} a_x sin\psi - \frac{m_f a}{I_f + m_f a^2} cos\psi u_1 - \frac{\varepsilon}{I_f + m_f a^2}\dot{\psi} \quad \mathbf{(4.26)}$$

4.1 Feedback Control Laws

For a development of feedback controllers, simple pendulum model is designed and using this model, optimal feedback controller and Lyapunov-based feedback controller are compared each other to attain accurate results.

4.1.1 Optimal feedback control law

As mentioned in the part of mass-spring system, optimal feedback control is a mathematical optimization method and it is applied to simple pendulum model. A special case of optimal controller that is called Linear Quadratic Regulator (LQR) is used and this controller aims minimizing the quadratic cost function.

Considering the system,

$$\dot{x} = Ax + Bu \quad \mathbf{(4.27)}$$

where

$$x = \begin{bmatrix} \theta \\ \dot{\theta} \\ \psi \\ \dot{\psi} \end{bmatrix} \qquad \dot{x} = \begin{bmatrix} \dot{\theta} \\ \ddot{\theta} \\ \dot{\psi} \\ \ddot{\psi} \end{bmatrix} \qquad u = \begin{bmatrix} \delta \\ M \end{bmatrix}$$

$$A = \begin{bmatrix} 0 & 1 & 0 & 0 \\ 0 & 0 & -\dfrac{\left(\dfrac{\mathrm{m_f a}}{\mathrm{m + m_f}}\right) I_2 F}{I_1 I_4 + I_2 I_3} & -\dfrac{(I_2 - I_4)\varepsilon}{I_1 I_4 + I_2 I_3} \\ 0 & 0 & 0 & 1 \\ 0 & 0 & -\dfrac{\left(\dfrac{\mathrm{m_f a}}{\mathrm{m + m_f}}\right) I_1 F}{I_1 I_4 + I_2 I_3} & -\dfrac{(I_1 + I_3)}{I_1 I_4 + I_2 I_3}\varepsilon \end{bmatrix} \qquad \mathbf{(4.28)}$$

$$B = \begin{bmatrix} 0 & 0 \\ -\dfrac{\left(I_2 \dfrac{\mathrm{m_f a}}{\mathrm{m + m_f}} - I_4 \left(\dfrac{m_f h_1}{m + m_f} + h_2\right)\right) F}{I_1 I_4 + I_2 I_3} & \dfrac{I_4}{I_1 I_4 + I_2 I_3} \\ 0 & 0 \\ -\dfrac{\left(I_1 \dfrac{\mathrm{m_f a}}{\mathrm{m + m_f}} + I_3 \left(\dfrac{m_f h_1}{m + m_f} + h_2\right)\right) F}{I_1 I_4 + I_2 I_3} & -\dfrac{I_3}{I_1 I_4 + I_2 I_3} \end{bmatrix} \qquad \mathbf{(4.29)}$$

$$\mathrm{I_1} = \mathrm{I} + \frac{\mathrm{mm_f}}{\mathrm{m + m_f}}\left(\mathrm{h_1}^2 - \mathrm{ah_1}\right) \qquad \mathrm{I_2} = \frac{\mathrm{mm_f}}{\mathrm{m + m_f}} a h_1$$

$$\mathrm{I_3} = \mathrm{I_f} + \frac{\mathrm{mm_f}}{\mathrm{m + m_f}}(a^2 - a h_1) \qquad \mathrm{I_4} = \mathrm{I_f} + \frac{\mathrm{mm_f}}{\mathrm{m + m_f}} a^2$$

State feedback control is designed as;

$$u = -Kx \qquad \mathbf{(4.30)}$$

To define the cost functional, *K* is designed as tradeoff between the response of the system and the control effort, and *u* is searched to minimize the index. The cost function,

$$J = \int_0^\infty [x^T(t) Q x(t) + u^T(t) R u(t)] dt \qquad \mathbf{(4.31)}$$

Here, *Q* and *R* are an n x n symmetric positive-semi definite weighting matrix, and an m x m symmetric positive-definite weighting matrix, respectively.

The optimal control gain matrix *K* is found by solving Riccati equation. The Algebraic Riccati Equation;

$$A^T P + PA + Q - (PB)R^{-1}(B^T P) = 0 \tag{4.32}$$

and the optimal state-feedback matrix gain *K* is

$$K = R^{-1}(B^T P) \tag{4.33}$$

As a hint, MATLAB's LQR command is [K, P, E] = lqr (A, B, Q, R) can be used so as to solve The Algebraic Riccati Equation [16].

4.1.2 Lyapunov-based control law

According to the theory of Lyapunov that is mentioned before, an appropriate Lyapunov function is determined for a single simple pendulum model. A candidate Lyapunov function for a system $\dot{x} = f(x)$ must provide the necessary conditions which are $V > 0$ and $\dot{V} \leq 0$.

Having the inputs from previous chapter, the candidate Lyapunov function;

$$\dot{v}_z = u_1 + \dot{\theta} v_x(t) \qquad\qquad \ddot{\theta} = u_2$$

$$V = \frac{q_1}{2} {v_z}^2 + \frac{q_2}{2}\theta^2 + q_3\left[\left(\frac{m_f a a_x}{I_f + m_f a^2}\right)(1 - cos\psi) + \frac{1}{2}\left(\dot{\theta} + \dot{\psi}\right)^2\right] \tag{4.34}$$

The time derivative of Lyapunov function;

$$\begin{aligned}\dot{V} = q_1 v_z \dot{v}_z + \dot{\theta}\left(q_2\dot{\theta} + q_3\ddot{\psi}\right) + q_3\ddot{\theta}\left(\dot{\theta} + \dot{\psi}\right) \\ + q_3\dot{\psi}[\left(\frac{m_f a a_x}{I_f + m_f a^2}\right) sin\psi + \ddot{\psi}]\end{aligned} \tag{4.35}$$

Substituting the control inputs and $\ddot{\psi}$ into Eq. (4.35), improved equation is derived;

$$\dot{V} = u_1\left(q_1 v_z - q_3 \frac{m_f a}{I_f + m_f a^2}(\dot{\theta} + \dot{\psi})cos\psi\right) + \dot{\theta}\left(q_1 v_z v_x + q_2\theta - q_3 \frac{m_f a a_x}{I_f + m_f a^2} sin\psi - q_3 \frac{\varepsilon}{I_f + m_f a^2}\dot{\psi}\right) - q_3 \frac{\varepsilon}{I_f + m_f a^2}\dot{\psi}^2 \quad \textbf{(4.36)}$$

The feedback laws;

$$u_1 = -T_1\left[q_1 v_z - q_3 \frac{m_f a}{I_f + m_f a^2}(\dot{\theta} + \dot{\psi})cos\psi\right] \quad \textbf{(4.37)}$$

$$u_2 = -T_2\dot{\theta} - [q_1 v_z v_x + q_2\theta - q_3 \frac{m_f a a_x}{I_f + m_f a^2} sin\psi - q_3 \frac{\varepsilon}{I_f + m_f a^2}\dot{\psi}] \quad \textbf{(4.38)}$$

where q_1, q_2, q_3, T_1 and T_2 are positive constants and when they are placed in Lyapunov function, they satisfy the conditions for the function;

$$\dot{V} = -T_1\left[q_1 v_z - q_3 \frac{m_f a}{I_f + m_f a^2}(\dot{\theta} + \dot{\psi})cos\psi\right] - T_2\dot{\theta}^2 - q_3 \frac{\varepsilon}{I_f + m_f a^2}\dot{\psi}^2 \quad \textbf{(4.39)}$$

4.2 Simulations

An article, which belongs to Mahmut Reyhanoglu, are utilized as base for physical parameters, which are used in this part. The initial conditions which are necessary to show time responses of the spacecraft are; $v_{x0} = 10000$ m/s, $v_{z0} = 350$ m/s, $\theta_0 = 2°$, $\dot{\theta}_0 = 0.57°$, $\psi_0 = 15°$, $\dot{\psi}_0 = 0°$. For the simulations, the fuel burn time is assumed as 660 s.

Table 4.1: Physical Parameters for Simple-Pendulum Model

Parameters	Value
$\boldsymbol{m}$	600 kg
$\boldsymbol{m_f}$	100 kg
$\boldsymbol{I}$	$720\ \mathrm{kg/m^2}$
$\boldsymbol{I_f}$	$90\ \mathrm{kg/m^2}$
$\boldsymbol{F}$	2300 N
$\boldsymbol{a}$	0.2 m
$\boldsymbol{h_1}$	0.3 m
$\boldsymbol{h_2}$	0.2 m
$\boldsymbol{\varepsilon}$	$0.19\ \mathrm{kgm^2/s}$

4.2.1 Linear quadratic regulator

Linear Quadratic Regulator, which is studied theoretically in section 4.1, is utilized so as to investigate the stability of the spacecraft. By using physical parameters, necessary matrices are edited;

$$A = \begin{bmatrix} 0 & 1 & 0 & 0 \\ 0 & 0 & -0.0050 & -0.00025 \\ 0 & 0 & 0 & 1 \\ 0 & 0 & -0.6987 & -0.0023 \end{bmatrix}$$

$$B = \begin{bmatrix} 0 & 0 \\ 0.7629 & 0.0014 \\ 0 & 0 \\ -1.4243 & -0.0013 \end{bmatrix}$$

The weighting matrices;

$$Q = \begin{bmatrix} 1 & 0 & 0 & 0 \\ 0 & 1 & 0 & 0 \\ 0 & 0 & 1 & 0 \\ 0 & 0 & 0 & 1 \end{bmatrix}$$

$$R = \begin{bmatrix} 10 & 0 \\ 0 & 0.01 \end{bmatrix}$$

The optimal control gain matrix K;

$$K = \begin{bmatrix} 0.3153 & 1.2211 & -0.3495 & -0.2697 \\ 0.7801 & 2.8642 & -0.6581 & 0.0878 \end{bmatrix}$$

The eigenvalues of the system matrix A-BK;

$$Ei = \begin{bmatrix} -0.3312 + 0.8233i \\ -0.3312 - 0.8233i \\ -0.3298 + 0.3295i \\ -0.3298 - 0.3295i \end{bmatrix}$$

4.2.2 Lyapunov-based controller

Physical parameters taken from Table 4.2 are utilized to write edited Lyapunov function and check the function whether providing the requirements or not.

Table 4.2: Necessary physical parameters of simple-pendulum model for Lyapunov function

Parameters	**Value**
$\boldsymbol{q_1}$	10^{-7}
$\boldsymbol{q_2}$	10
$\boldsymbol{q_3}$	10^{-2}
$\boldsymbol{T_1}$	10^{3}
$\boldsymbol{T_2}$	1

$$V = 5 * 10^{-8} {v_z}^2 + 5\theta^2 + 6.991 * 10^{-2}(1 - cos\psi) + 5 * 10^{-3}\left(\dot{\theta} + \dot{\psi}\right)^2$$

$$\dot{V} = -10^{-4} v_z + 2.128\left(\dot{\theta} + \dot{\psi}\right) cos\psi - \dot{\theta}^2 - 2.0213 * 10^{-5}\dot{\psi}^2$$

$$u_1 = -10^{-4} v_z + 2.128\left(\dot{\theta} + \dot{\psi}\right) cos\psi$$

$$u_2 = -\dot{\theta} - [2.128 * 10^{-3} v_z v_x + 10\theta - 6.991 * 10^{-3} sin\psi - 2.0213 * 10^{-5}\dot{\psi}]$$

4.2.3 Graphics of simple-pendulum model

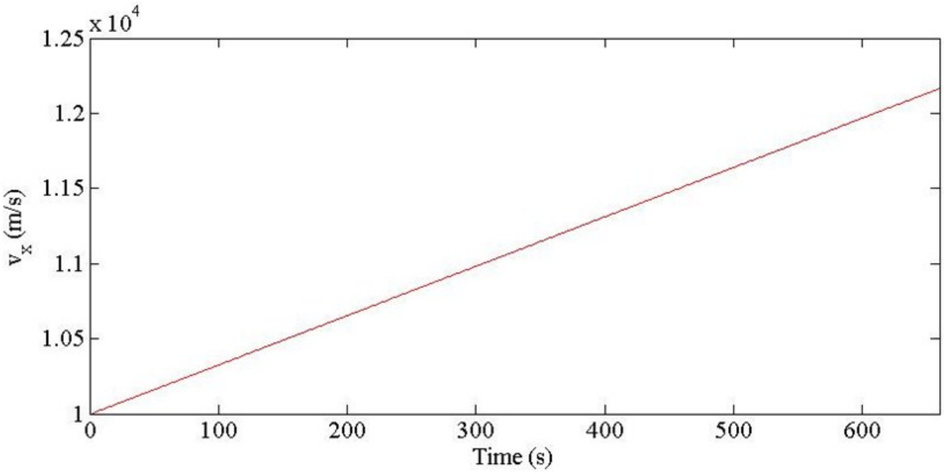

Figure 4.2: Change of axial component of velocity with respect to time for simple-pendulum system

5. CONCLUSIONS AND RECOMMENDATIONS

The effects of propellant slosh in a rigid tank of any vehicle have been crucial over the motion. Particularly for space vehicles, the sloshing term is a great factor for a spacecraft's motion and the stability. The free surface of liquid allied to container exhibits different types of motion due to the energy exchange between interacting modes. Based on this energy exchange, the motion may result in the inner resonance case and it may drift into a state of chaos that means when sloshing starts to occur because of the peak acceleration, structural damages become evitable.

To minimize the damages in container, liquid's motion must be controlled effectively. By using computer programmes or carrying out experiments over the liquid's attitude in a case of sloshing, dynamic loads over the structure may be predicted. In spite of getting nearly accurate results, these methods have been very complex since the beginning. In this thesis, to investigate the dynamic loads over the tank and spacecraft, for propellant of vehicle, a transform, which is from liquid fuel to rigid inner masses, is utilized. This transform comes true by designing equivalent mechanical systems, which are appropriate to parameters of liquid fuel.

Firstly, equivalent mechanical models are investigated under excitations in order to show the effects of external forces and moments. Lateral and pitching excitations over the space vehicle are studied and then, change in the force and moment equations are derived theoretically.

Secondly, multi-mass-spring system are designed as an equivalent mechanical system with a non-sloshing part. Kinetic energy and potential energy are derived with the help of oscillation of inner rigid masses and then Lagrangian form are composed. This Lagrangian form is used to derive the equations of motion of spacecraft in the absence of external forces and moments. After deriving the equations, parameters based on an article of Reyhanoglu & Hervas are utilized to demonstrate the stability graphics. For this mass-spring system, Linear Quadratic Regulator and Lyapunov-based Controller are studied to simulate the stability of the spacecraft. LQR does not give accurate results since the system's time-varying situation is nondisposable. A and B matrices in control theory does not enable the conditions because the poles of A are not controllable through B. Therefore, LQR cannot be used to simulate the results of mass-spring system. A candidate Lyapunov function is chosen as an alternative control theory to show the simulations. It gives accurate and appropriate results in demonstration. What's more, the mass-spring system is designed by changing the number of inner-masses and demonstrated the results of two model. Main purpose is to show the effects of the number of the masses over spacecrafts. As one can see from the graphics in Chapter 3, there is not a significant alteration between the results of systems.

Ultimately, simple-pendulum model are planned as an equivalent mechanical system to demonstrate fuel sloshing. There is no potential energy because the gravitational effects are ignored. Therefore, Lagrangian form are composed of only kinetic energy in the absence of external forces and moments. Like in the mass-spring model, parameters of liquid fuel are taken from an article, which is belong to Hervas & Reyhanoglu, and they are utilized to make a simulation about the stability of spacecraft. Linear Quadratic Regulator and Lyapunov-based controller are studied theoretically to demonstrate the stability graphics. As a conclusion, LQR does not give accurate result in the transverse component of the velocity of space vehicle and it fails with a steady-state error. A chosen candidate Lyapunov function succeeds to stabilize the pitch and slosh dynamics.

REFERENCES

[1] **Lehman, M.** (1963). This High Man: The Life of Robert H. Goddard, Farrar Straus, New York

[2] **Abramson, H.N.** (1969). Slosh suppression report, NASA, Washington DC, SP-8031

[3] **Ebrahimian, M., Noorian, M. A., and Haddadpour, H.** (2014). Equivalent mechanical model of liquid sloshing in multi-baffled containers, Sharif University of technology, Tehran, Iran, June 9

[4] **Adler, J. M., Lee, M. S., and Saugen, J.D.** (1991). Adaptive control of propellant slosh for launch vehicles, General Dynamics Space Systems Division, San Diego, California

[5] **Dong, K., Qi, N. M., Guo, J. J., and Li, Y. Q.** (2008). An estimation approach for propellant sloshing effect on spacecraft GNC, IEEE, Harbin Institute of technology, Harbin, China

[6] **Dodge, F. T., and Garza, L. R.** (1967). Experimental and theoretical studies of liquid sloshing at simulated low gravity, Journal of Applied Mechanics, San Antonio, Texas

[7] **Reyhanoglu, M., and Hervas, J. R.** (2012). Nonlinear dynamics and control of space vehicles with multiple fuel slosh modes, Control Engineering Practice, Elsevier, May 21

[8] **Cui, D. L., Yan, S. Z., Guo, X. S., and Gao, R. X.** (2014). Parametric resonance of liquid sloshing in partially filled spacecraft tanks during the powered-flight phase of rocket, Aerospace Science and Technology, Elsevier, March 18

[9] **Xue-lia, Z., Xian-sheng, L., and Yuan-yuan, R.** (2012). Equivalent mechanical model for lateral liquid sloshing in partially filled tank vehicles, Hindawi Publishing Corporation, Mathematical Problems in Engineering, Volume 2012, Article ID 162825

[10] **Conaway, R. W., and Spindler, J. S.** (1967). Anti-slosh media for fuel tanks, United States Patents, NO: US3349953 A, dated 31 October 1967

[11] **Chun, S. E.** (2011). Anti sloshing apparatus, United States Patents, NO: US8708190 B2, dated 17 May 2011

[12] **Ha, D. J.** (2007). Anti-sloshing structure for LNG cargo tank, United States Patents, NO: US8235242 B2, dated 4 December 2007

[13] **Schwager, B. A., and Curran, P. J.** (1996). Fuel sloshing detection, United States Patents, NO: US5765121 A, dated 4 September 1996

[14] Meirovitch, L., and Kwak, M. K. (1989). State equations for a spacecraft with maneuvering flexible appendages in terms of quasi-coordinates, ASME, Appl Mech Rev. vol 42, no 11, Part 2

[15] Ibrahim, R. A. (2005). Liquid sloshing dynamics theory and applications, Wayne State University, Department of Mechanical Engineering, Cambridge University Press

[16] Hespanha, J. P. (2005). Lecture notes on LQR/LQG controller, University of California Santa Barbara, February 27

[17] Ge, S. S. (n.d.). Lyapunov design, The National University of Singapore, Department of Electrical and Computer Engineering, EOLSS Publications, data retrieved January 2015

[18] Freeman, R. A., and Kokotovic, P. V. (1996). Robust nonlinear control design: State-Space and Lyapunov Techniques, Birkhauser Boston, Modern Birkhauser Classics

[19] Strogatz, S. H. (2000). Nonlinear dynamics and chaos, Perseus Books Publishing, LLC, United States of America

[20] Hervas, J. R., and Reyhanoglu, M. (2012). Control of a spacecraft with time-varying propellant slosh parameters, 12^{th} International Conference on Control, Automation and Systems, October 17-21, ICC, Jeju Island, Korea

CURRICULUM VITAE

Name Surname: Merve ŞAHİN

Place and Date of Birth: Eminönü, İstanbul, 26/09/1990

Address: Vatan cad. Hüsrevpaşa sok. NO: 41/6 Fatih/İstanbul

E-Mail: mervesahin90@gmail.com

B.Sc.: Yıldız Technical University, Department of Physics, July 2012

PUBLICATIONS, PRESENTATIONS AND PATENTS ON THE THESIS:

- Şahin, M., Cihan, M., and Kaya, M. O., Model and control problem for space vehicles with propellant slosh, Recent Advances in Space Technologies, 16-19 July 2015, İstanbul